depth	length	Au g/t	Cu %	Mo ppm
161.10m–162.60m	(1.50m)	0.21	0.069	116
163.30m–173.10m	(9.80m)	0.20	0.043	69
205.90m–222.90m	(17.00m)	0.06	0.062	120
322.70m–325.70m	(3.00m)	0.09	0.364	63

In the mineralized zone as mentioned above, the section from 210.40 m to 219.00 m (8.60 m) has chalcopyrite-pyrite bearing quartz vein, in addition to this, it should be emphasized that the copper mineralized zone was intersected toward to the bottom part (from 322.70 m to 325.70 m).

(5) Drilling Hole MJM-5 (0° –50°, 350.60 m)

The hole is situated in 620 m of direct distance from the location of MJM-1 (MJM-3) to the eastward.

The purpose of this hole is to confirm the underneath horizon of the high geochemical anomalous zone (Cu 1,000–3,000 ppm) where shows the second highest value (the highest zone was already explored by MJM-1, MJM-3), in OMRD survey.

The Hole is occupied only by turbidute, which shows compact rock facies.

The size of gravels are from those more than one metre to less than few centimeteres of sandstone and mudstone whose shapes are from angular to subangular, while a matrix shows black-gray color and muddy-clayey facies.

Regarding the alteration, weak silicification, calcitization and argillization are common together with weak pyritization in some part, throughout of the hole.

Strong pyrite dissemination occur in undermentioned depth, however no remarkable copper occurrence has been recognized.

depth	length	Au g/t	Cu %	Mo ppm
21.50m– 35.50m	(14.00m)	0.03	0.005	4
157.40m–179.00m	(21.60m)	0.02	0.005	3
335.80m–350.60m	(14.80m)	0.01	0.004	5

Among these, the last portion (the bottom of the hole) is an intense pyrite disseminated zone accompanying with strong argillization.

(6) MJM–6 (–90° (vertical), 302.60 m)

The purpose of the hole was to clarify both the thicknesses of the Pinosuk Gravels and the blank area underneath the Gravels, which have obstructed further exploration.

Geology of the hole was the Pinosuk Gravels whose thickness is continuing from the surface to the depth of 161.30 m, and peridotite downward.

The Pinosuk Gravels consist of gravels of angular – subangular of its size from one meter maximum to less than thirty centimeters and sandy matrix.

The kinds of gravels are various sedimentary rocks, igneous rocks and metamorphosed rocks, which are originally delivered from the surrounding area.

It can be derided for two kinds of layers, a loose layer (loose Pinosuk Gravels) which is distributed from surface to the depth of 60.80 m with partially receiving strong weathering, and a solid and hard layer (solid Pinosuk Gravels) distributing to the bottom of the hole. However, the differences of rock facies such as the kind of gravels and matrix can not be distinguished.

In the gravels, pyrite and chalcopyrite has accasionally been found in places as a form of disemination.

The peridotite underneath the Pinosuk Gravels has suffered alterations such as serpentinization and pyritization throughout accompanying with fracturing and argillization.

Near the top of peridolite at the depth of 167.20 m, fine chalcopyrite and molybdenite dissemination in the clayey shear zone of its length of 30 cm has been intersected.

The results of referencial chemical analysis is as follows;

Au (gr/t)	Cu %	Mo ppm
0.37	0.50	18

The results of chemical analysis of the weak mineralized zone, other than these above mentioned, are as follows;

depth	length	Au g/t	Cu %	Mo ppm
172.40 m –177.40 m	(5.00 m)	0.00	0.021	9
227.40 m – 231.90 m	(4.50 m)	0.05	0.071	8

(7) MJM–7 (70° –50°, 350.20 m)

The purpose of the hole was to investigate the possibility of mineralization underlying the Pinosuk Gravels in the northern blank area of the location of MJM–2 and MJM–4 holes, because the porphyry copper type mineralization was comfirmed in the peridotite of the hole of MJM–6.

The geology was peridotite until 12.20 m from the surface and after a shear zone adamellite-porphyry until 40.00 m, then gray-dark grey colored, compact hornfels throughout the hole.

And further, adamellite-porphyry at the depth of 59.50 m with its width of 2.80 m and micro-diorite at the depth of 233.10 m with its width of 11.47 m were encountered.

The alteration such as silicification, carbonatization and weak pyritization were observed throughout the hole.

The mineralizations in hornfels at the depth of 93.60 m and in biotite-micro diorite which was mentioned above were observed as the strong dissemination of pyrite with very low grade of copper.

The result of the referenced analysis was as follows;

depth	length	Au g/t	Cu %	Mo ppm
93.60 m – 96.80 m	(3.20 m)	0.0	0.025	3
233.10 m –244.60 m	(11.50 m)	0.0	0.026	4

(8) MJM–8 (270° –50°, 351.00 m)

The remarkable IP anomaly obtained in this phase, was detected in the resistivity area with lower than 70ohm-m around the survey point of 500W on the line E and F situated in the west bank of the Bambangan Creek.

Among these anomalies, the one figure on the line E shows 3.0% – 4.0% in PFE with its depth of about 100 m from surface.

The drilling hole was to confirm the chalacteristics of the anomalies at the location of 300W on the Line-F of SIP survey line, about 100 m east of the holes of MJM–2 and MJM–4.

The geology of the hole was that through the loose Pinosuk Gravels until the depth of 107.80 m, enter into adamellite porphyry, then peridotite from 293.00 m to the bottom of the hole (see Fig. 46).

The upper part of the adamellite-porphyry shows strong oxidation and bleaching with shearing and a little strong silicification. From depth of 180.00 m in the adamellite-porphyry, silicification and pyritization develope, and after this zone the intensity of alteration become rather weak.

From the depth of around 207.30 m where a fault fractured zone was passed, a strong pyritized zone accompanying chalcopyrite dissemination was intersected.

The zone between the depth of 240.00 m and 260.90 m is strongly silicified and the mineralization of chalcopyrite dissemination and network are observed, showing the clear nature of porphyry-copper. After this zone, the hole entered into the weakly mineralized zone with a small scale zone of better copper grade.

The mineralized zones can be divided into three zones, i.e., the depths of 180.00 m – 180.60 m (6.00 m wide), 196,80 m – 197.20 m (0.70 m) and 207.30 m – 291.10 m (83.80 m).

The better parts distinguished by eye are the following three parts, i.e., 240.00m–260.60m (20.60 m wide), 282.80 m – 283.50 m (0.70 m) and 284.60 m – 286.60 m (2.00 m).

The referenced assay grades by spot sampling are as follows (now the samplings and the chemical analysis are being done by the Geological Survey of Malaysia, Sabah);

depth	length	Au g/t	Cu %	Mo ppm
240.00 m – 243.60 m	(0.60 m)	0.2	0.40	30
254.20 m – 254.80 m	(0.60 m)	0.4	1.13	16
270.50 m – 271.20 m	(0.70 m)	0.0	0.19	195

The periodotite is suffered serpentinization, chloritization, talc, weak silicification and carbonatization through out, the marcasite and molybdenite minerals can also be observed near the parts of adamellite-porphyry mineralized zone.

(9) MJM–9 (–90° (vertical), 401.10 m)

The mineralized zone being expected underneath of the Pinosuk Gravels was aimed as well as the purpose of the hole of MJM–7.

The geology of the hole was that after passing the thick Pinosuk Gravels until 270.70 m entered into peridotite, then through the sheared zone between 329.40 m and 335.10 m, the reddish brown-gray colored hornfels was encountered until the bottom of the hole.

The thickness of the Pinosuk Gravels occuring in this hole reaches more than 400 m if adding the exposed layers in eastward steep cliff.

The Pinosuk Gravels as described in the clause of MJM–6 can be devided into two layers such as the loose Pinosuk Gravel until 48.30 m and then the solid Pinosuks.

The gravels and matrix part show the same rock facies as those in the other hole.

Serpentinization is commonly observed in the peridotite. The hornfels portions show silicification between the depth of 383.90 m and the bottom of the hole.

The referenced chemical analyses were made for the mineralized zone bearing minor amount of chalcopyrite disseminations, as shown below;

depth	length	Au g/t	Cu %	Mo ppm
291.90 m – 296.00 m	(4.10 m)	0.62	0.144	68
326.30 m – 327.80 m	(1.50 m)	0.52	0.094	7
335.10 m – 348.90 m	(13.80 m)	0.10	0.142	39
380.30 m – 395.80 m	(15.50 m)	0.04	0.067	9

(10) MJM–10 (70° –50°, 351.90 m)

The purpose of the hole is to confirm the geology and the occurence of mineralization underneath the Pinosuk Gravels in the blank area of northern part of MJM–7.

The geology was the Pinosuk Gravels until 243.80 m and to the depth of 330.90 m, then entered into spilite and hornfels until the bottom. (see Fig. 46).

The Pinosuk Gravels have a rock facis of the loose Pinosuk Gravels as bearing argillized soft matrix part, however judging from the occurence of the Pinosuk Gravels in the cliff in front of the drilling site, it should be recognized as the solid Pinosuk Gravels.

As seen on geological profile (Map 46–10), the thickness of the Pinosuk Gravels in this area is vertically more than 290 m, from the top level of surface to the lower bottom in the drilling hole.

The gravels of the layer consists of the same as those of the other holes. However, in the lower horizon of the Gravels, the gravels and matrixes are of peridotite adamellite rock facies.

It is assumed that the drilling site situates in the close adjacent area of the Kinabalu admellite batholith and the intrusive bodies of in immediate south of the batholith, from which the gravaels of the Pinosuk Gravels were supplied.

The alterations of serpentinization, silicification, carbonatization and chloritization are observed in peridotite, however the intensities are rather weak. Magnetite mineral is also detected throughout the hole.

The spilite and hornfels occur repeatedly in the bottom part of the hole after peridotite, with the alteration of silification, chloritization and epidotization in part. The pyritization is very weak in local. No pyritization occurs in peridotite.

LEGEND


PG Pinosuk Gravels (loose)

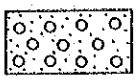
PG Pinosuk Gravels (compact)

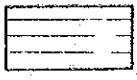
Td Turbidite

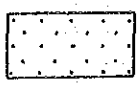
Ss Sandstone

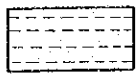
St Siltstone


Mt Mudstone (Sh) (Shale)

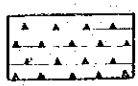
Hf Hornfels

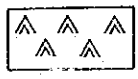
Sp Spilite


Md Microdiorite

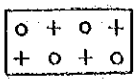
Ap Adamellite porphyry (Ad) (Adamellite)

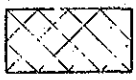
Pt Peridotite

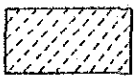
arg argillized

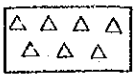
bre brecciated (frag) (fragmented)

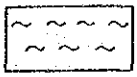
shr sheared


silic silicified

Abbreviations

bi ; biotite	pyr ; pyrrhotite	gr ; grained
cal ; calcite	arg ; argillized	grvl ; gravel
chlo ; chlorite	bg ; bearing	imp ; impregnation
cly ; clay	blchd ; bleached	lns ; lens
gt ; garnet	bld ; boulder	netwk ; network
qz ; quartz	bre ; brecciated	oxd ; oxidized
srp ; serpentine	cls ; clastic	strg ; stringer
tlc ; talc	diss ; dissemination	vlt ; veinlet
cp ; chalcopyrite	fin ; fine	wthd ; weathered
limo ; limonite	flt ; fault	xeno ; xenolith
moly ; molybdenite	fract ; fractured	(vp) ; (very poor)
		(p) ; (poor)
py ; pyrite	frag ; fragmented	(m) ; (moderate)
		(a) ; (abundant)

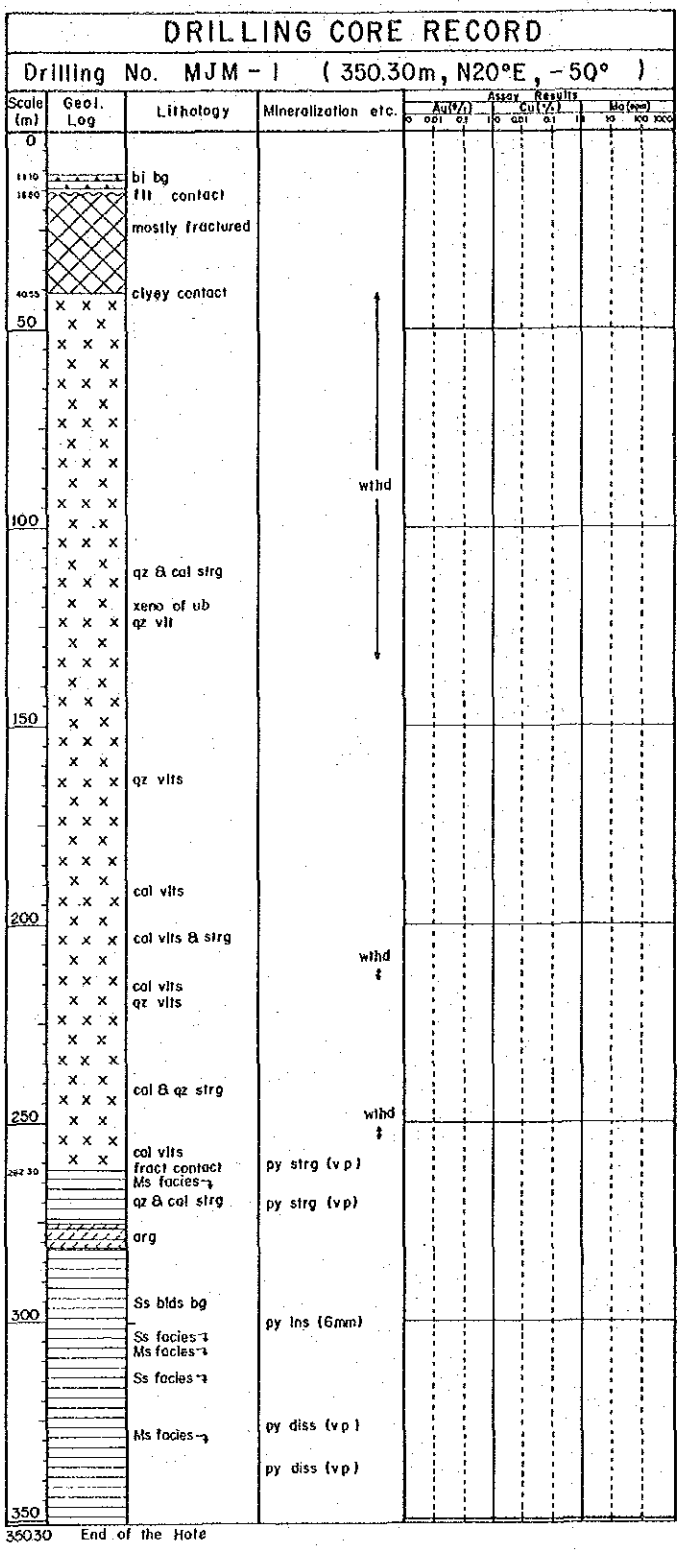

Fig. 45–1 Columnar Section of Drill Hole (MJM–1)

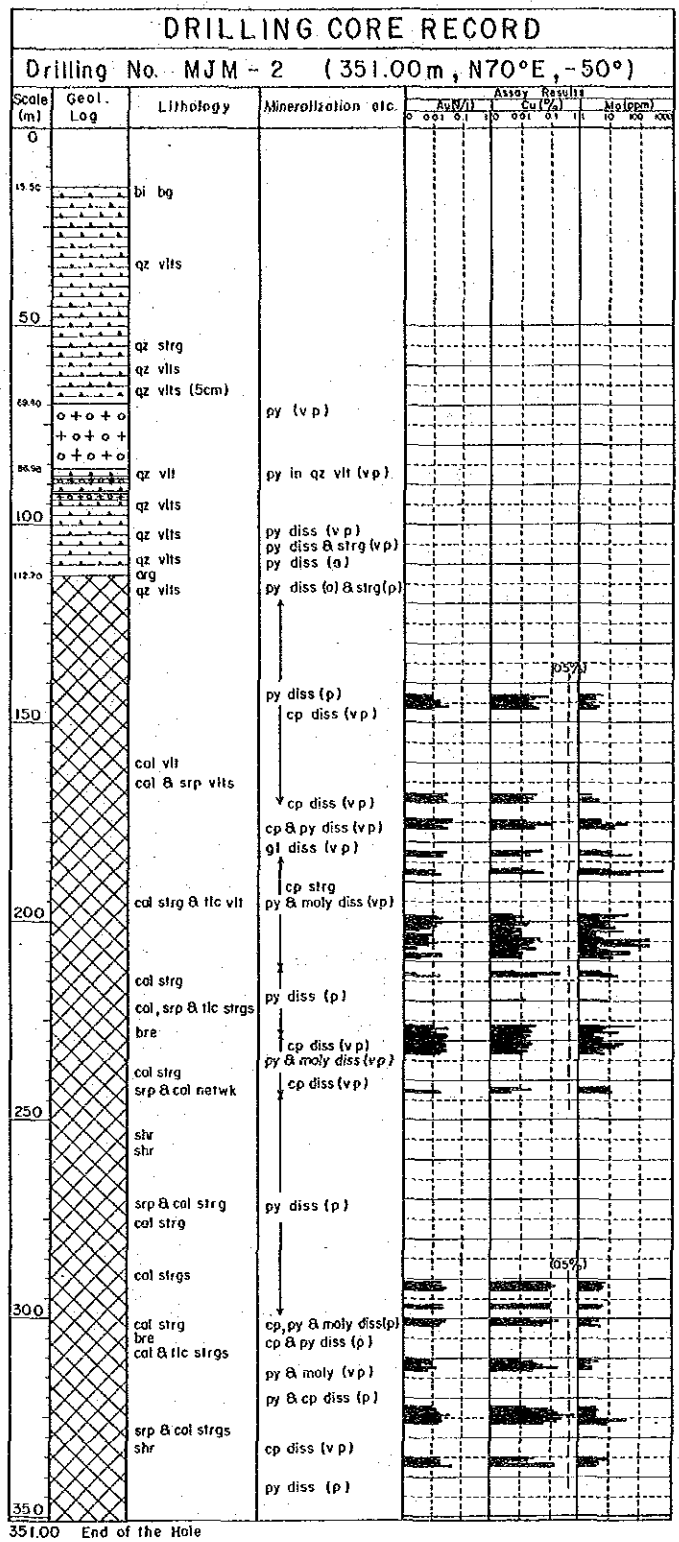

Fig. 45–2 Columnar Section of Drill Hole (MJM–2)

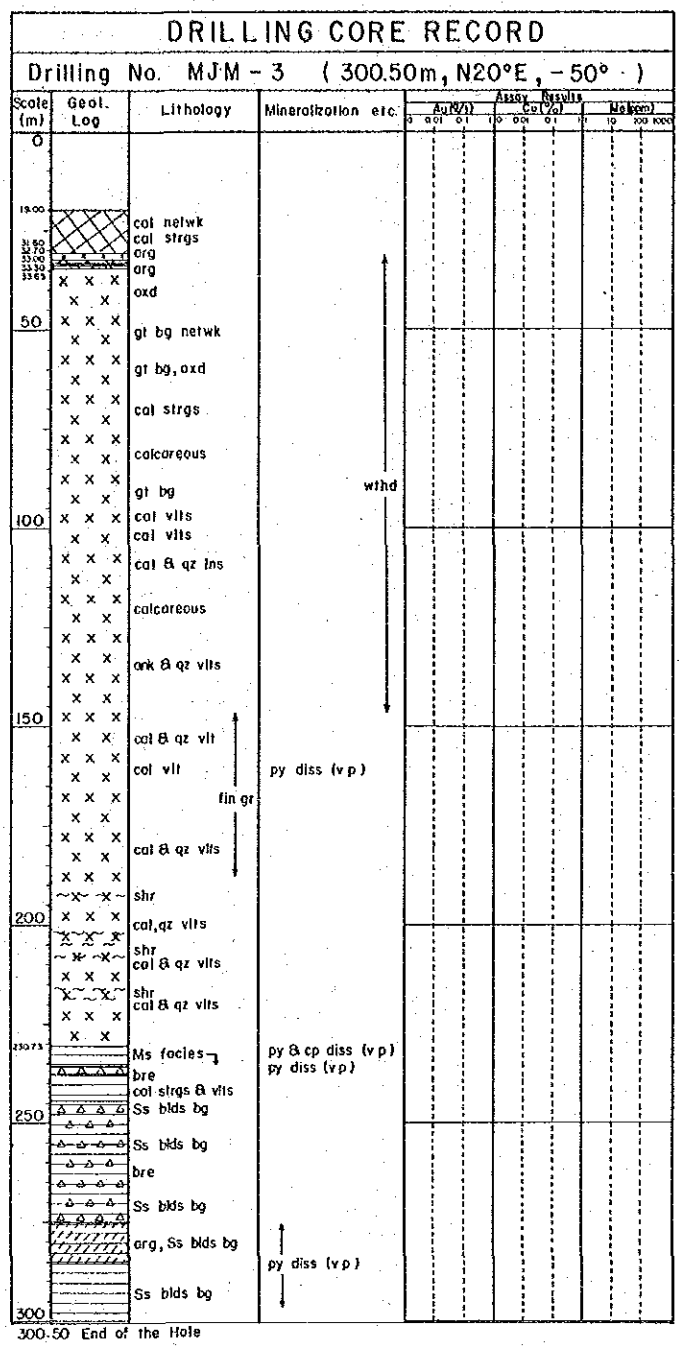

Fig. 45–3 Columnar Section of Drill Hole (MJM–3)

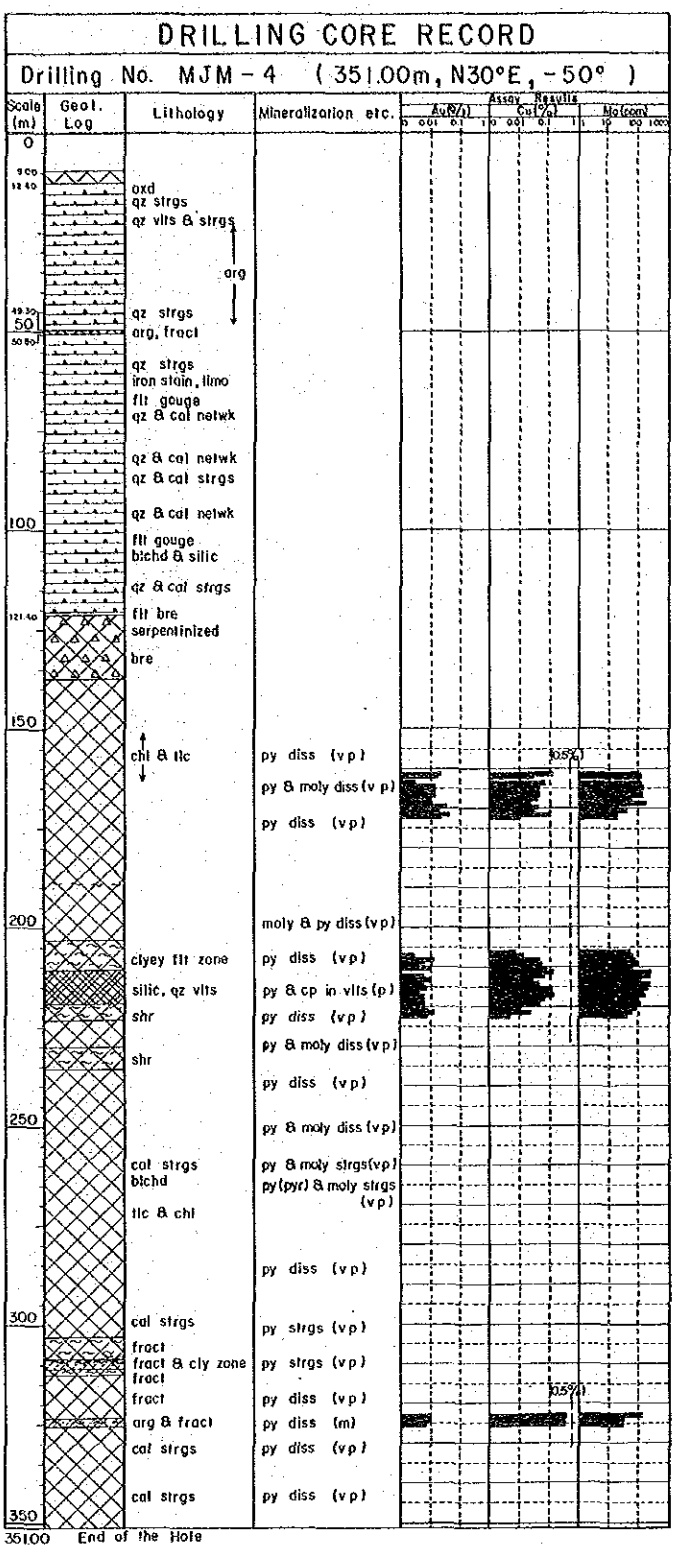

Fig. 45–4 Columnar Section of Drill Hole (MJM–4)

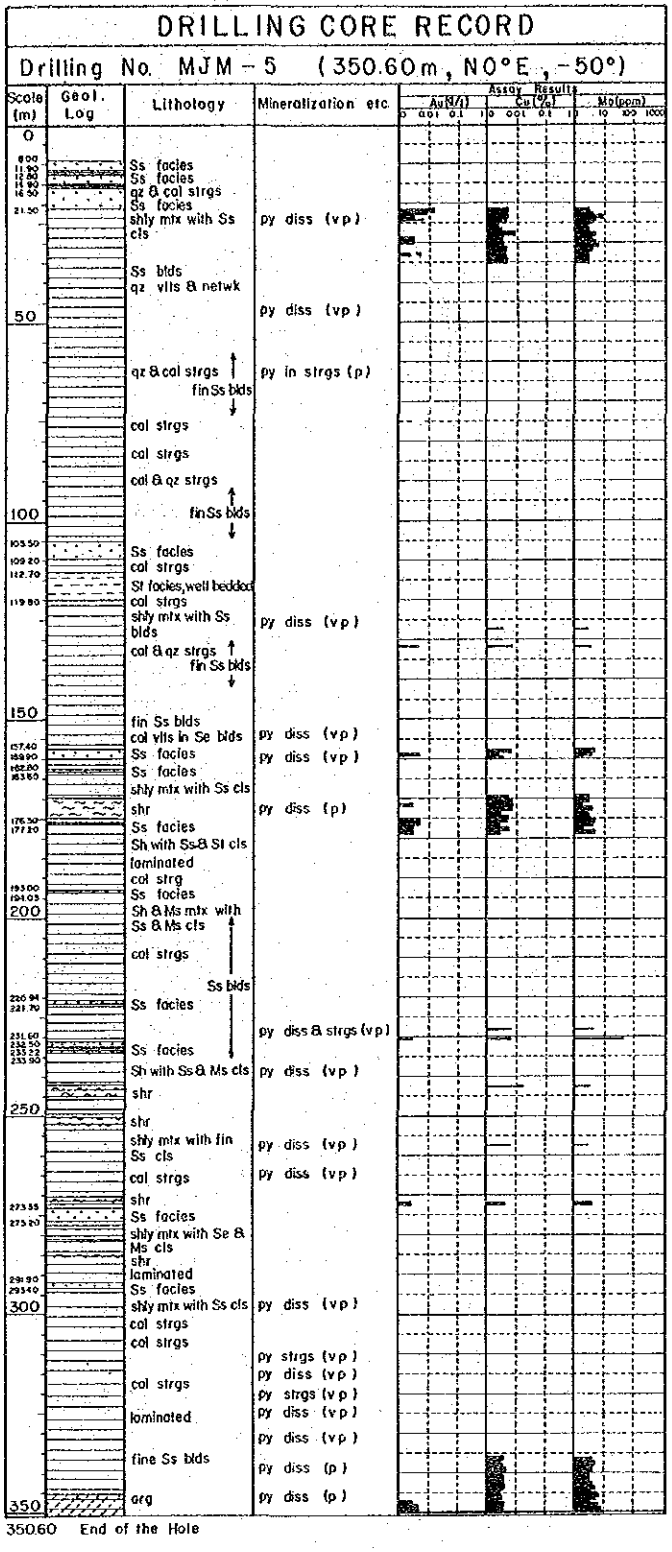

Fig. 45－5 Columnar Section of Drill Hole (MJM－5)

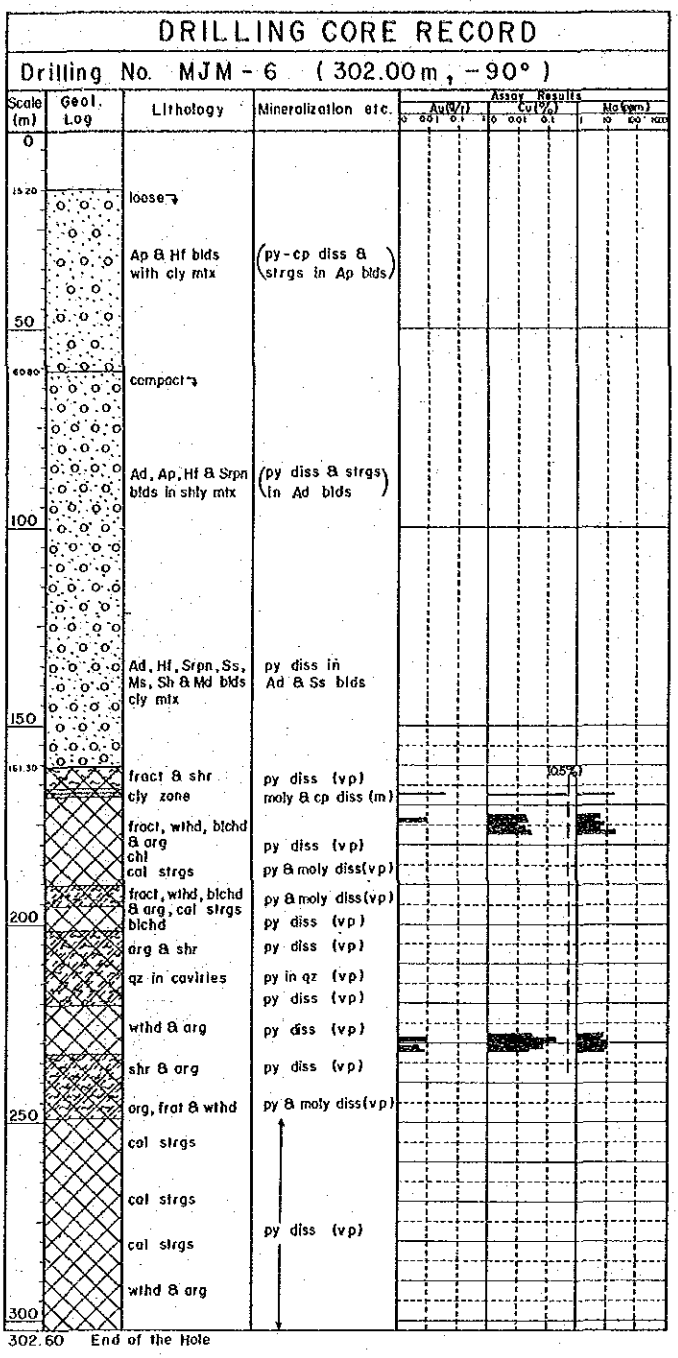

Fig. 45–6 Columnar Section of Drill Hole (MJM–6)

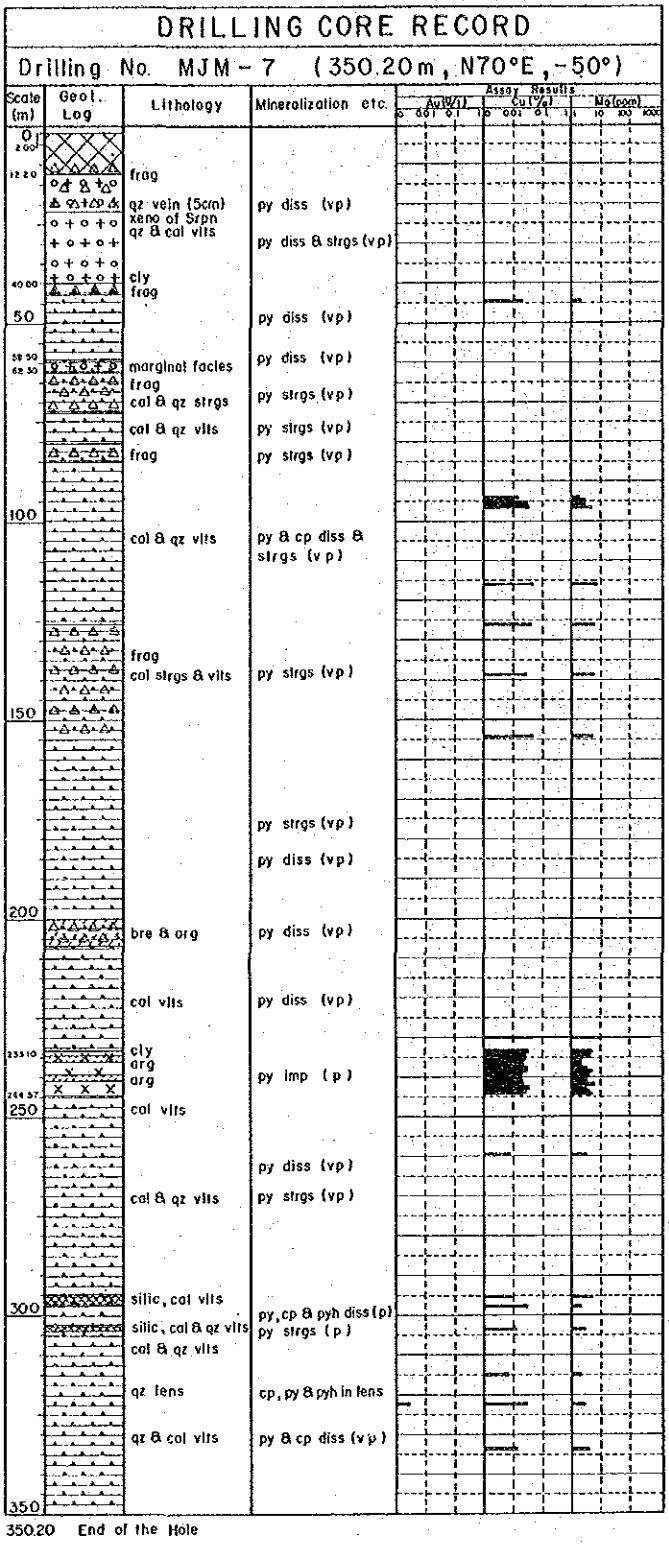

Fig. 45–7 Columnar Section of Drill Hole (MJM–7)

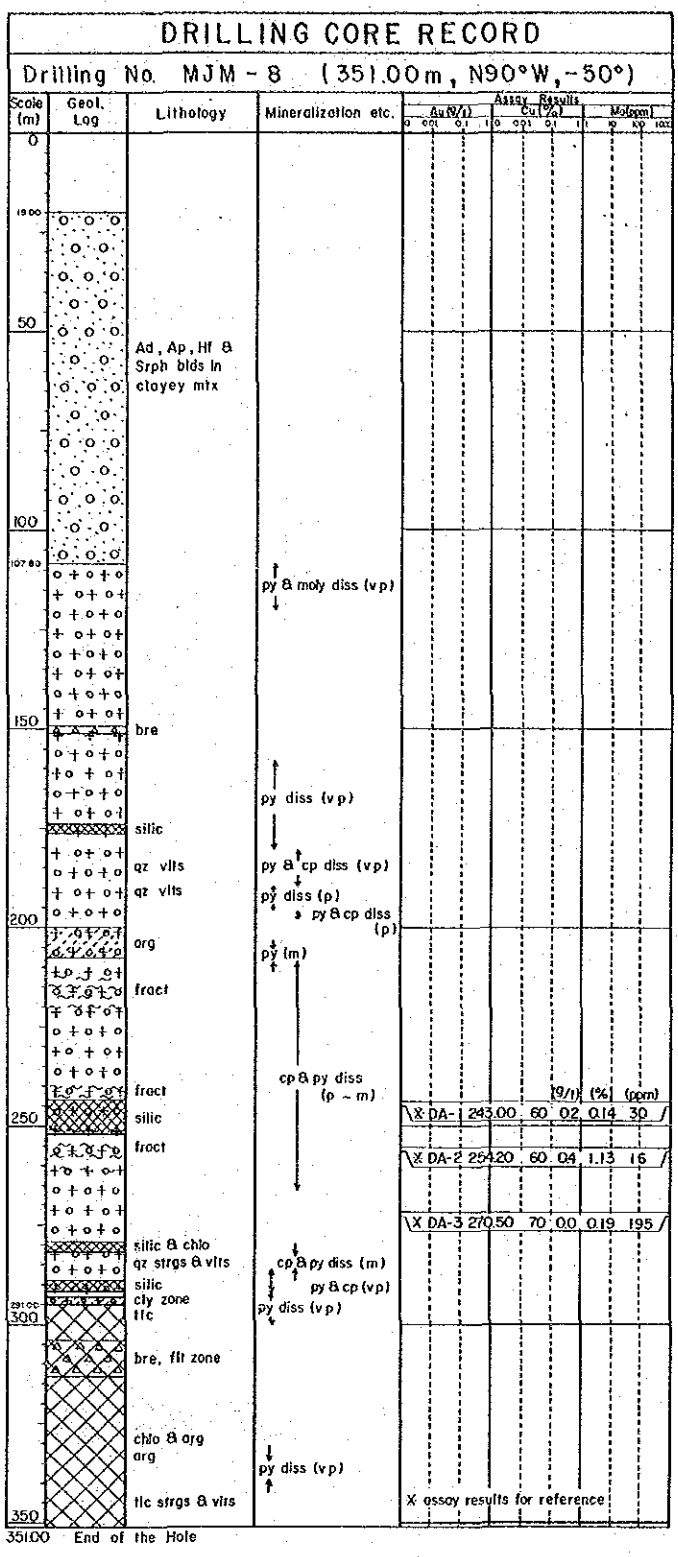

Fig. 45–8 Columnar Section of Drill Hole (MJM–8)

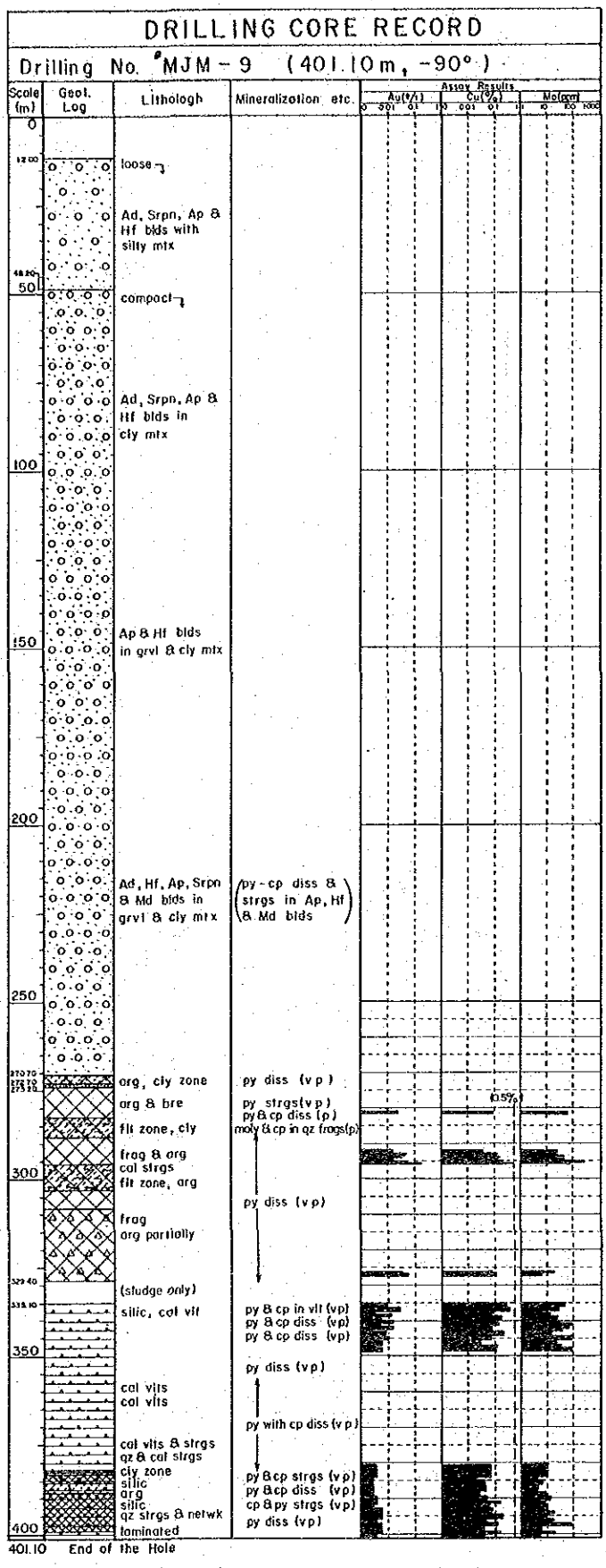

Fig. 45–9 Columnar Section of Drill Hole (MJM–9)

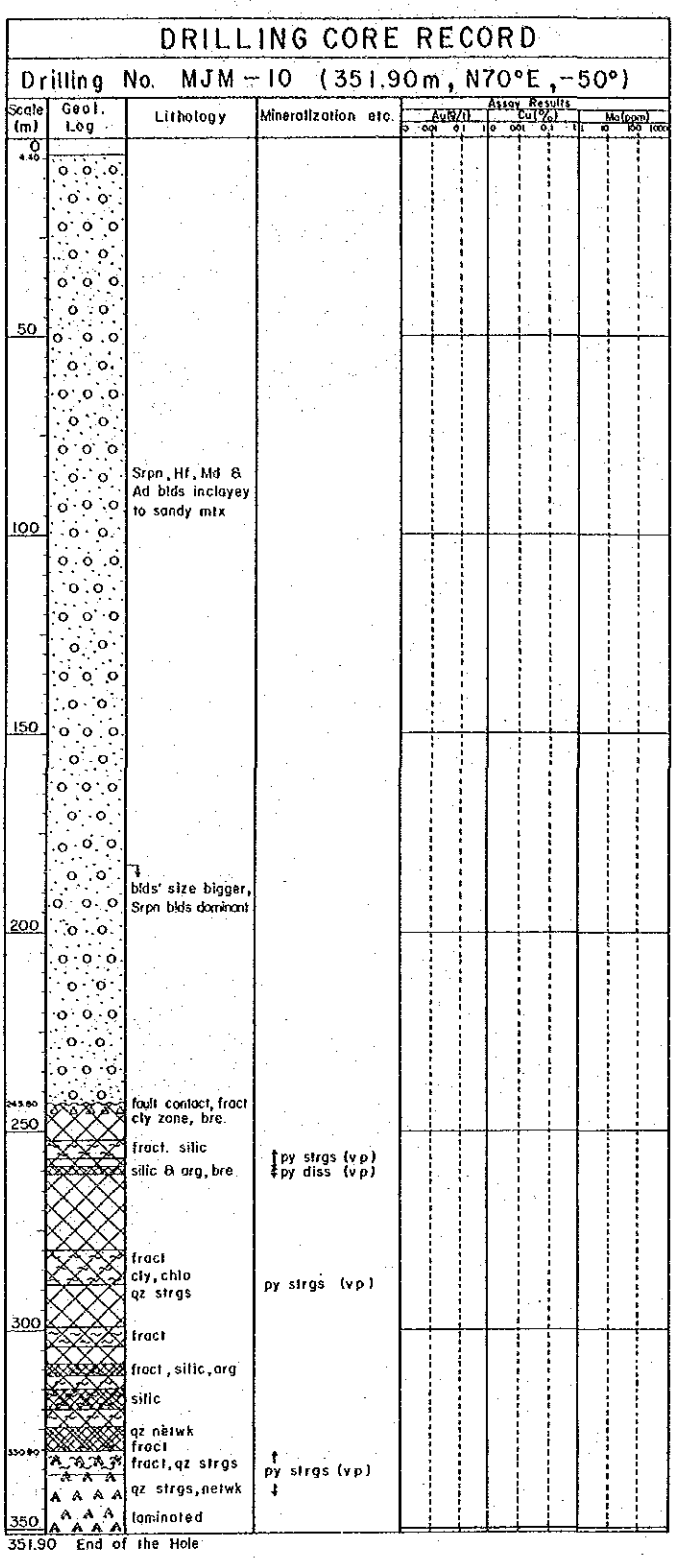

Fig. 45－10 Columnar Section of Drill Hole (MJM－10)

MJM－8　Adamellite Porpyry fractured zone

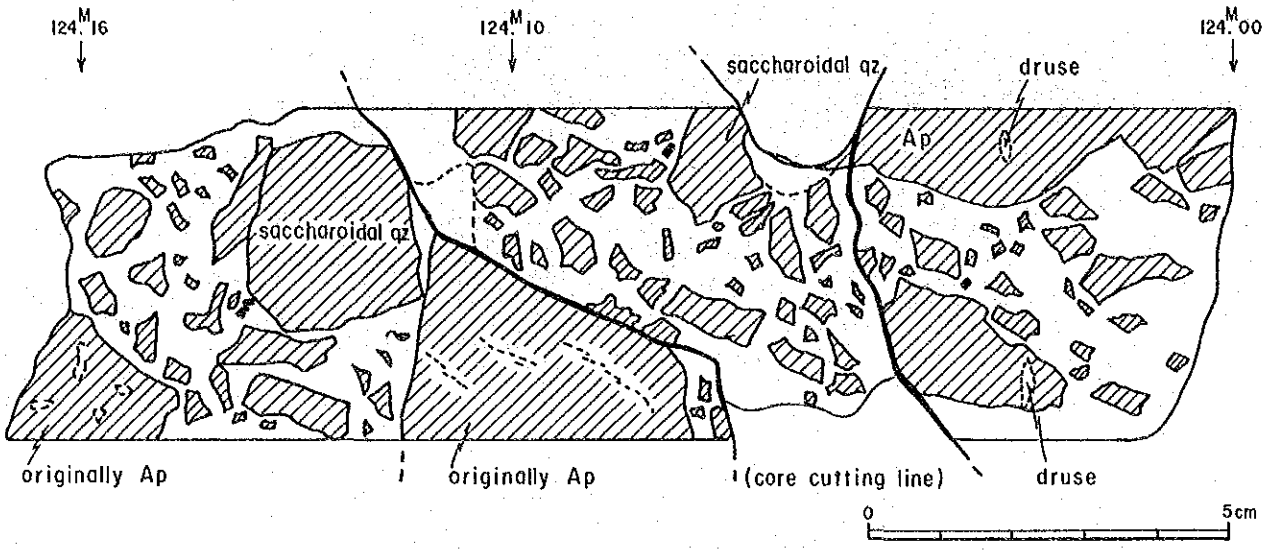

matrix is green arkose sand (fine to medium size)
among small angular pebble, and some of them shows pale eartly color

MJM－10

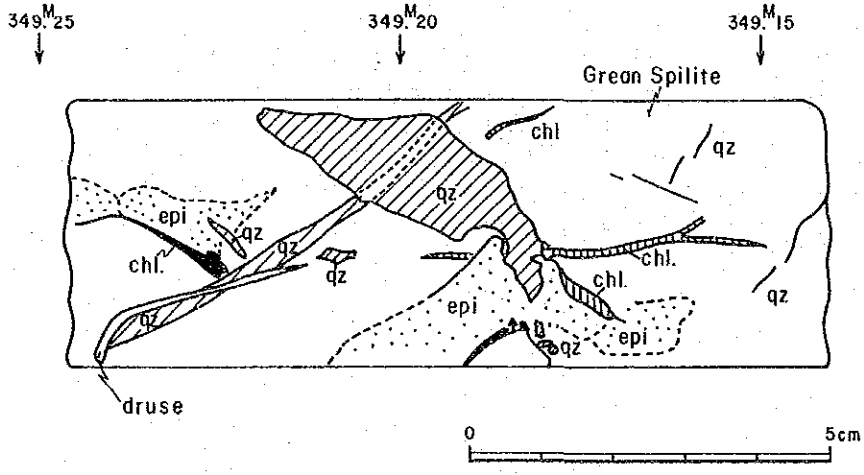

abbreviations ; qz－quartz, chl－chlorite,
epi－epidote
Ap－Adamellite porphyry

Fig. 46　Sketch of Drill Core

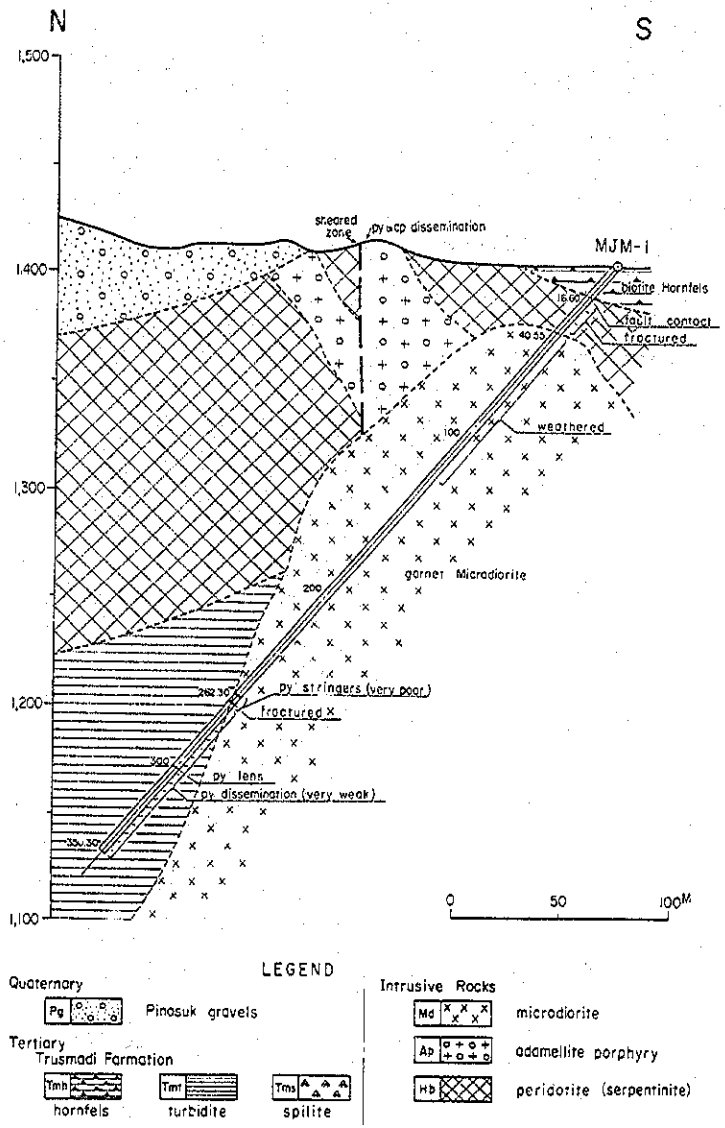

Fig. 47–1 Geological Section of Drill Hole (MJM–1)

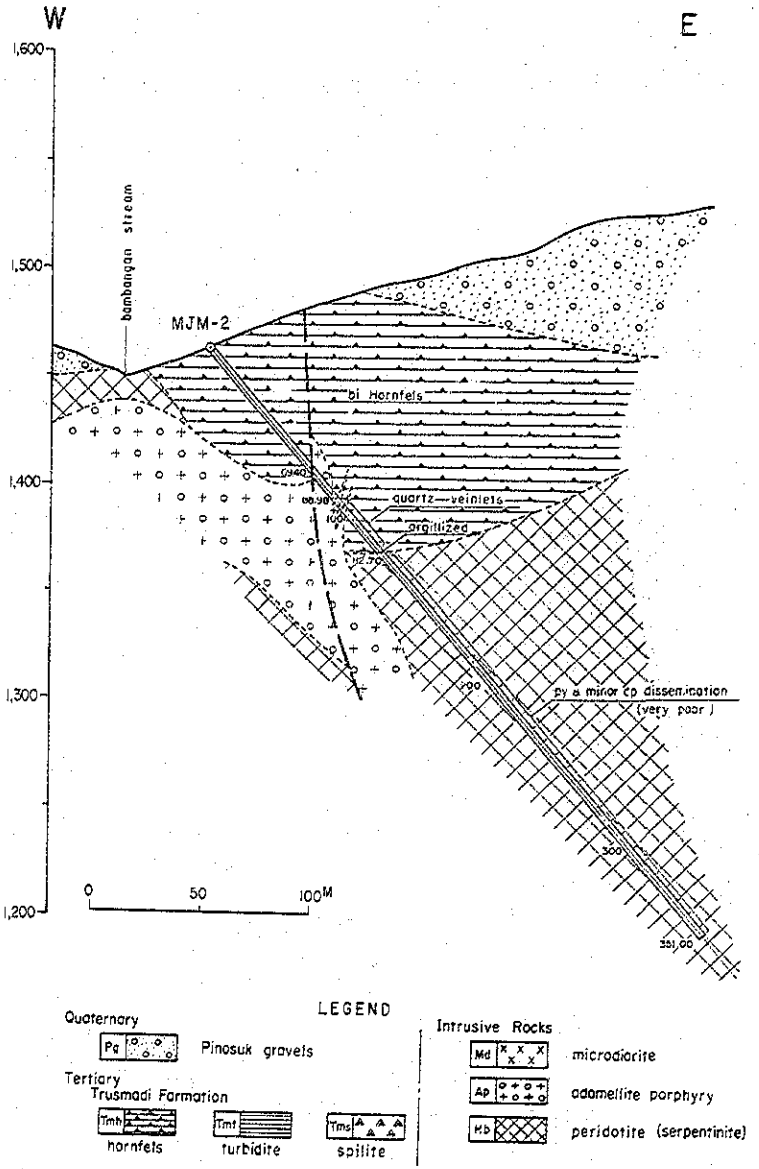

Fig. 47–2 Geological Section of Drill Hole (MJM–2)

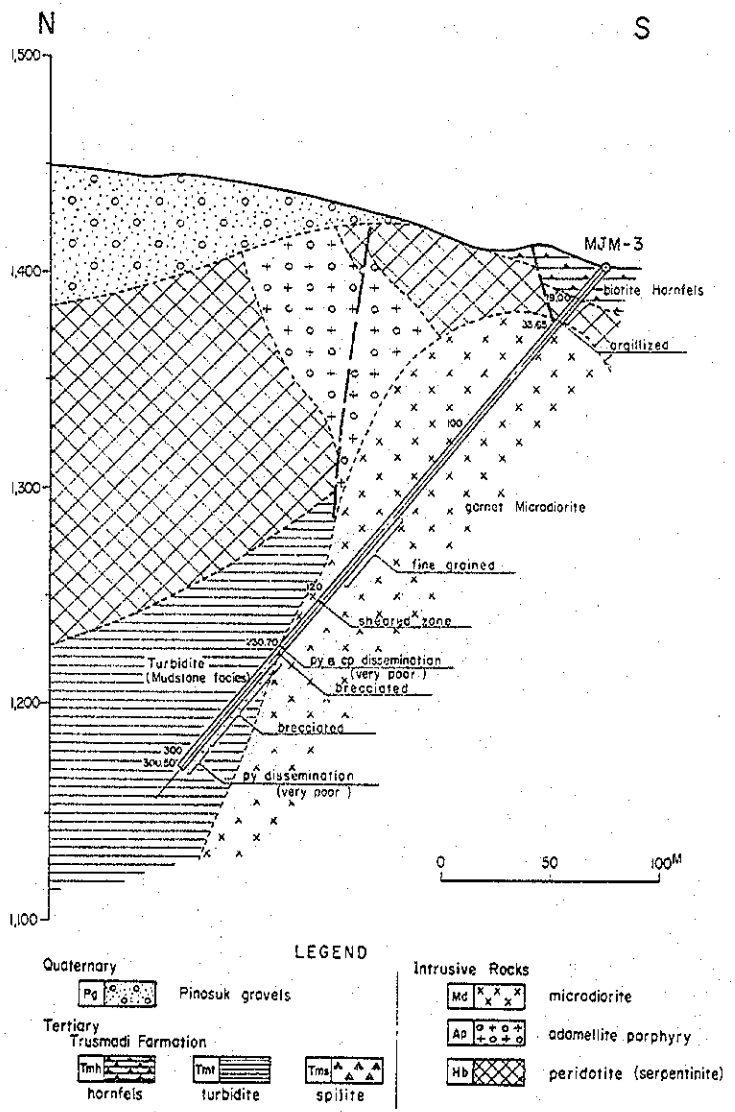

Fig. 47–3 Geological Section of Drill Hole (MJM–3)

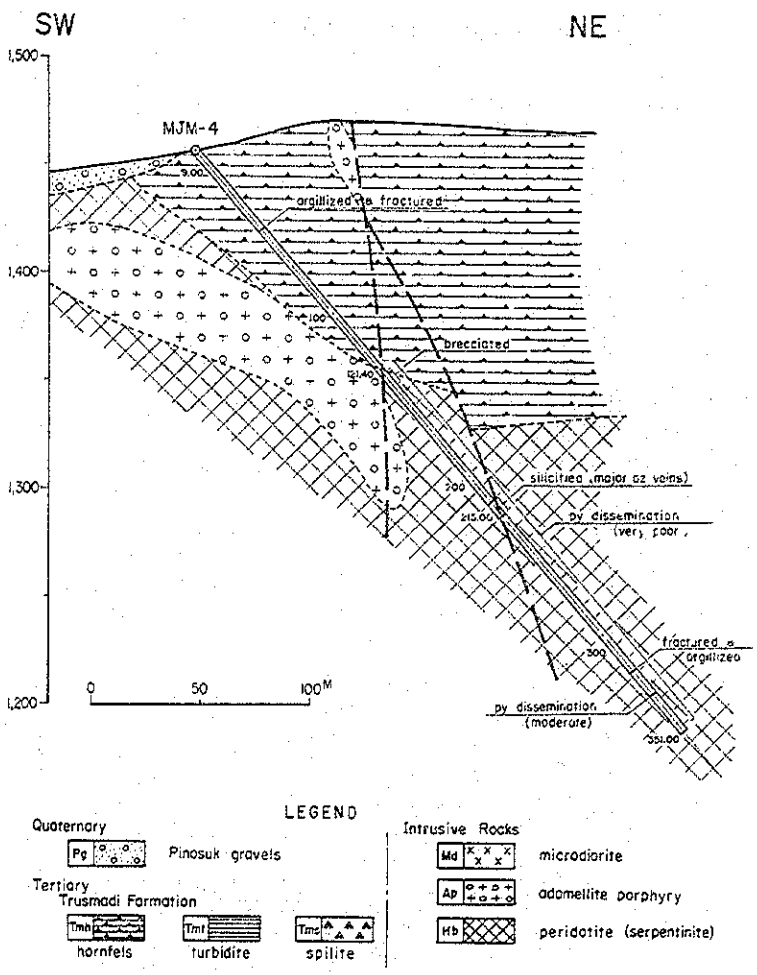

Fig. 47–4 Geological Section of Drill Hole (MJM–4)

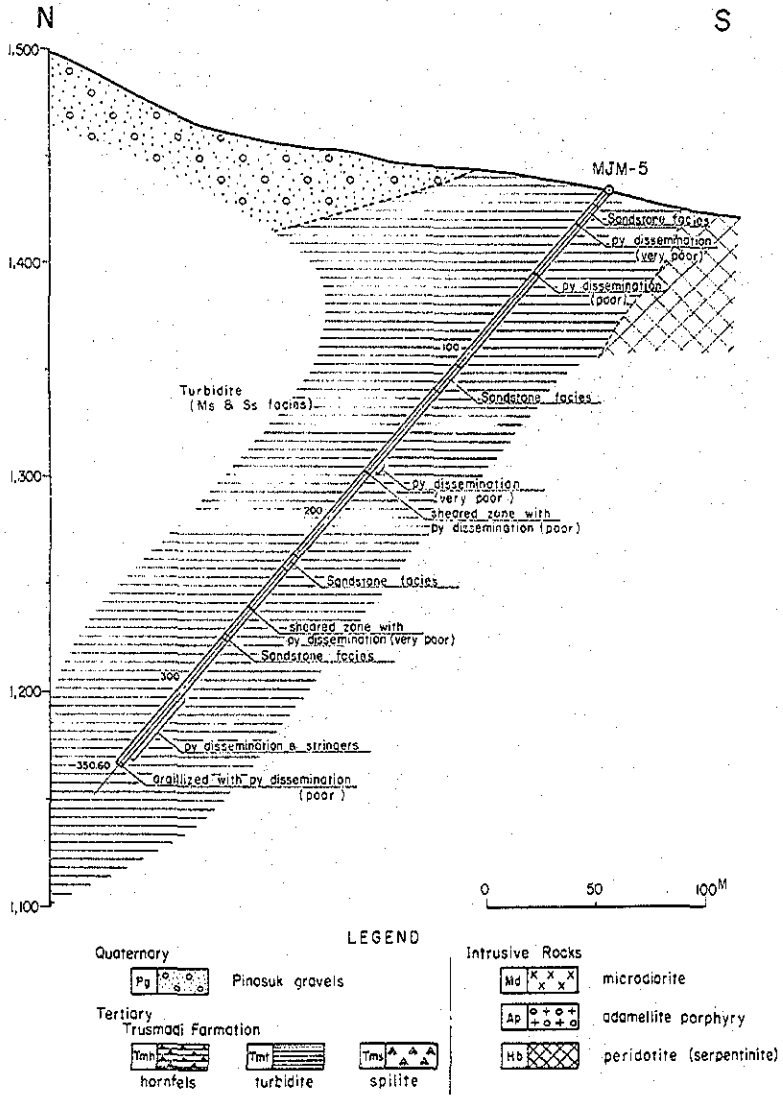

Fig. 47–5 Geological Section of Drill Hole (MJM–5)

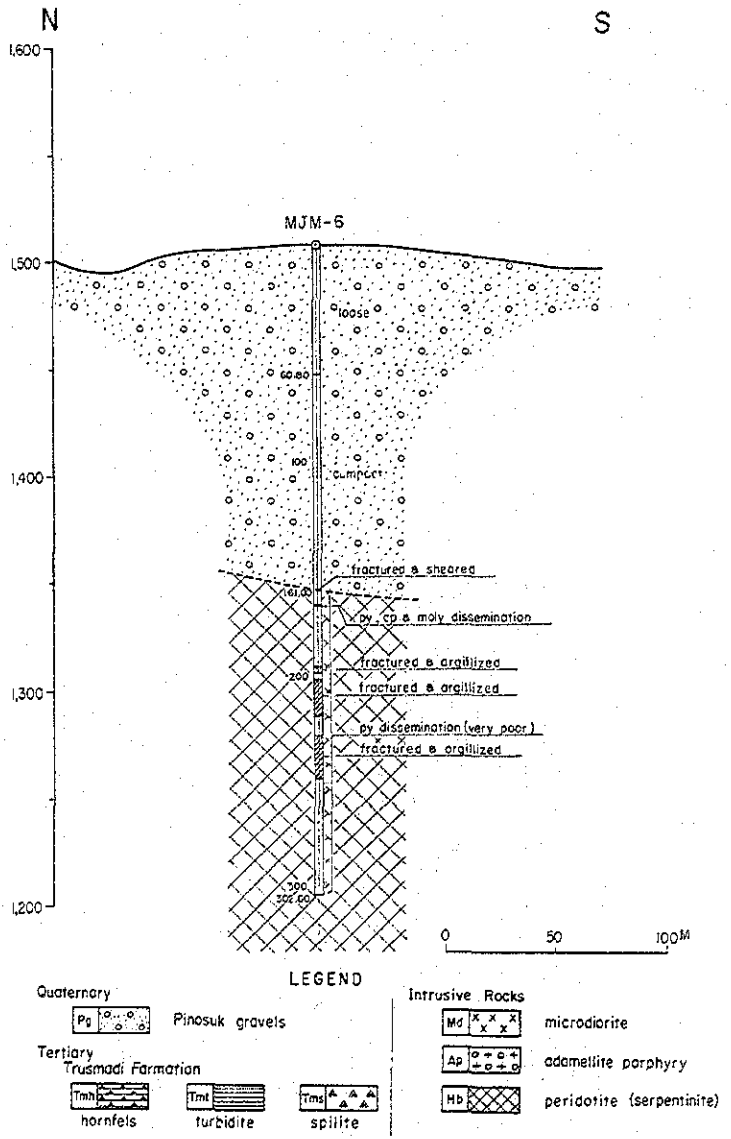

Fig. 47–6 Geological Section of Drill Hole (MJM–6)

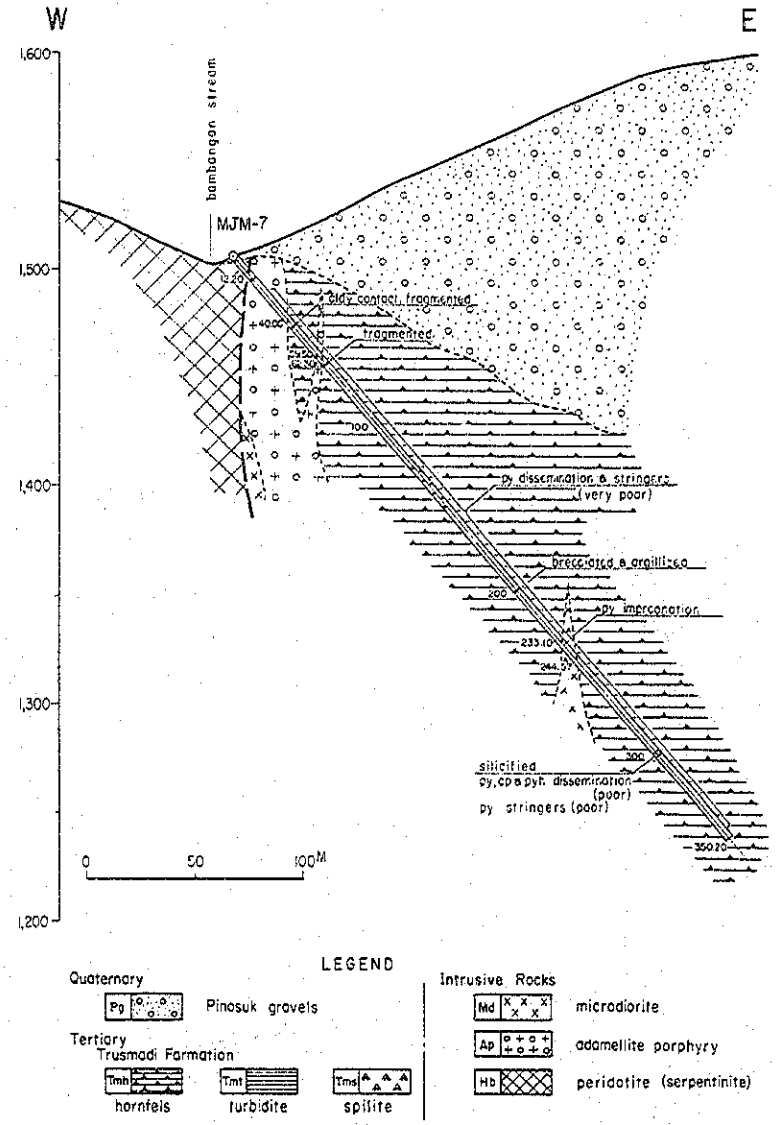

Fig. 47–7 Geological Section of Drill Hole (MJM–7)

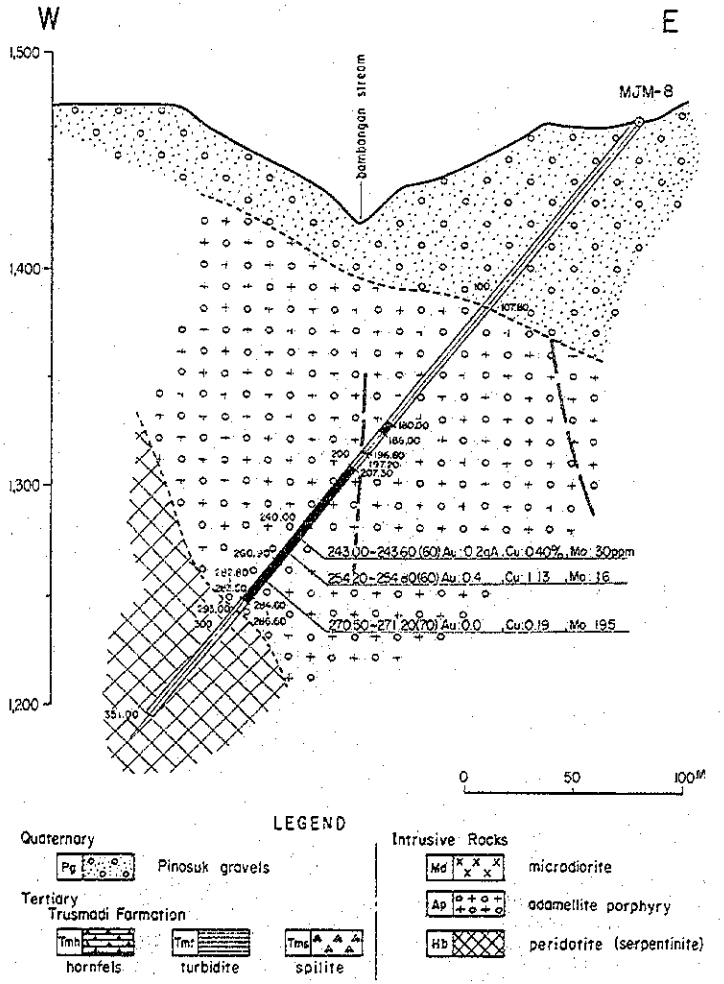

Fig. 47–8 Geological Section of Drill Hole (MJM–8)

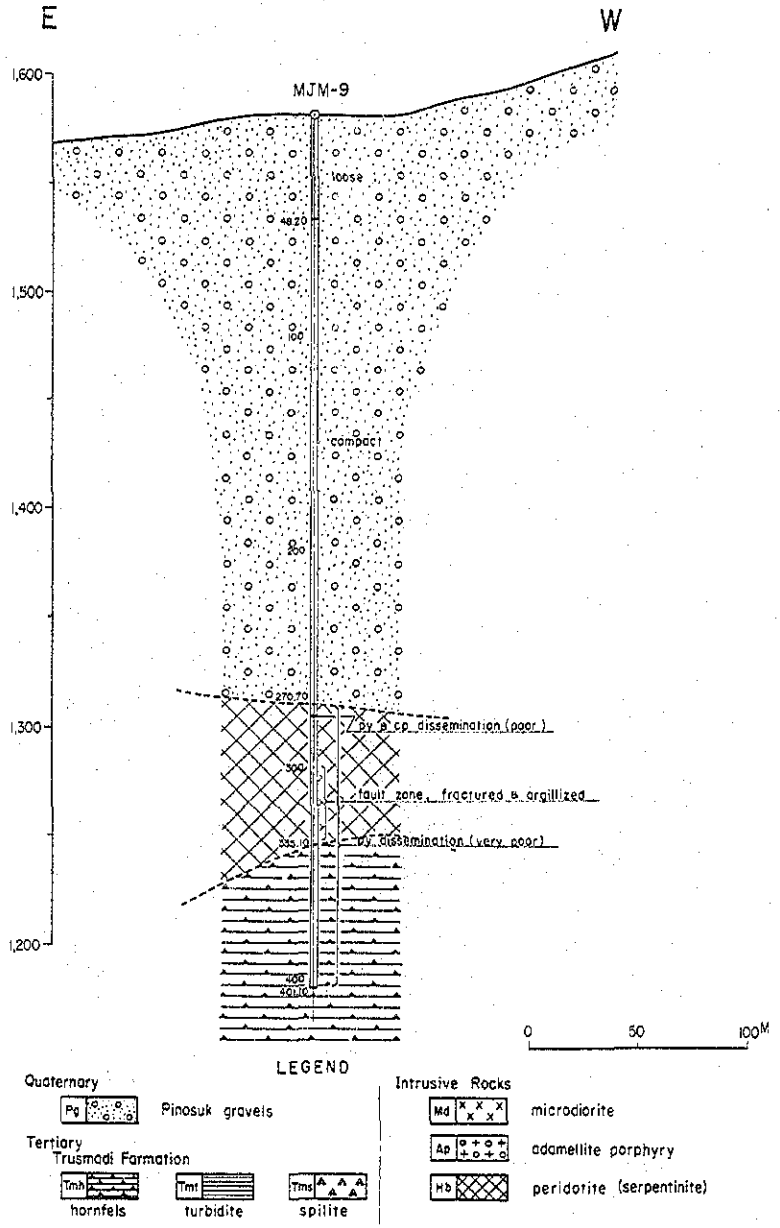

Fig. 47–9 Geological Section of Drill Hole (MJM–9)

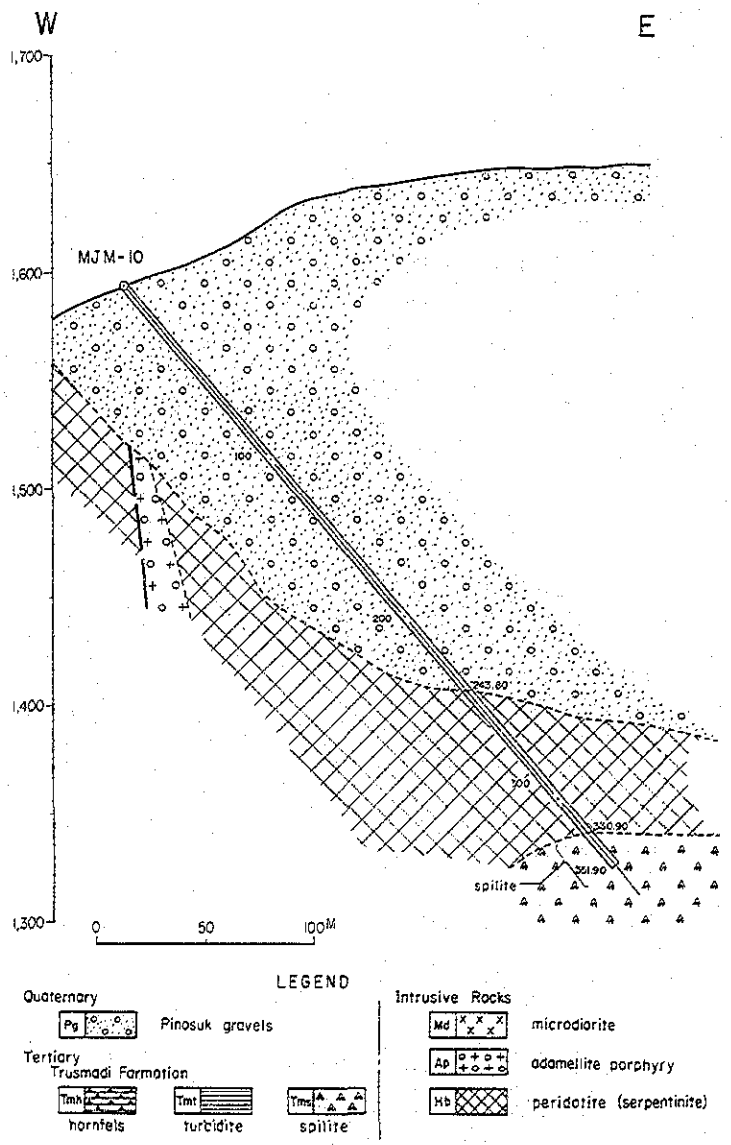

Fig. 47–10 Geological Section of Drill Hole (MJM–10)

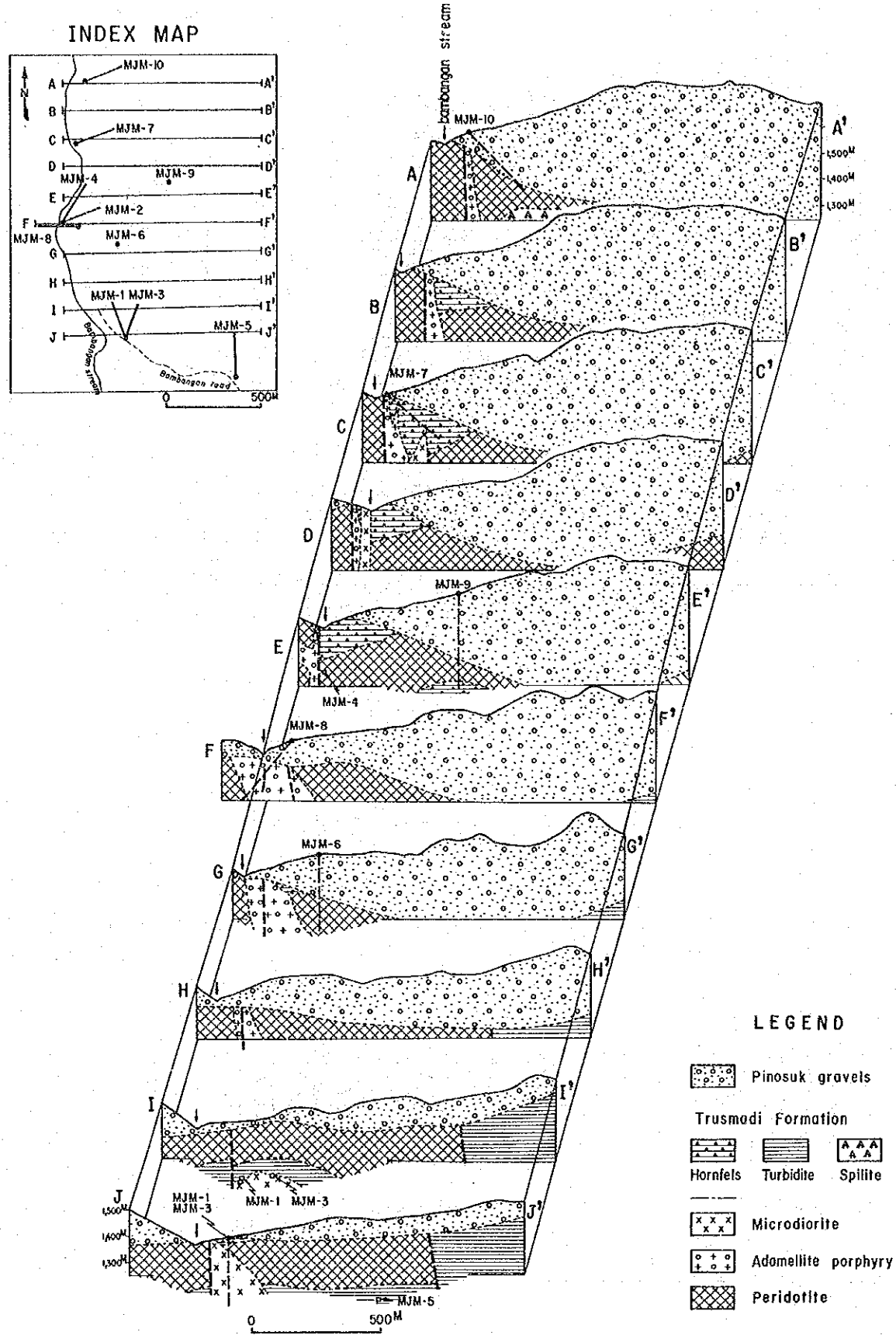

Fig. 48 Schematic Geological Section in "a" Area

3–2–2 Intrusive Rocks in the Drilling Holes

As mentioned before, the Bambangan Creek is a fault valley, along which the adamellite porphyry and microdiorite have intruded.

The drill holes of MJM-1, 2, 3, 7 and 8 locating near the Bambangan Creek have intersected these dykes with a small scale.

The normative compornents of a fresh adamellite core at 75.00 m depth of MJM-2 hole and a microdiorite core at 178.80 m depth of MJM-1 hole fall in the areas of quartz monzonite (adamellite) and granodiorite, as shown in Fig. 49.

The analytical data made by OMRD and Kirk (1978) for the adamellite porphyry and granodiorite, distributing in the area of the Mamut ore bodies shows some variations in the chemical composition in places. Therefore, the correlation between the Mamute Mine and the Bambangan area is difficult due to the limited data in the Bambangan.

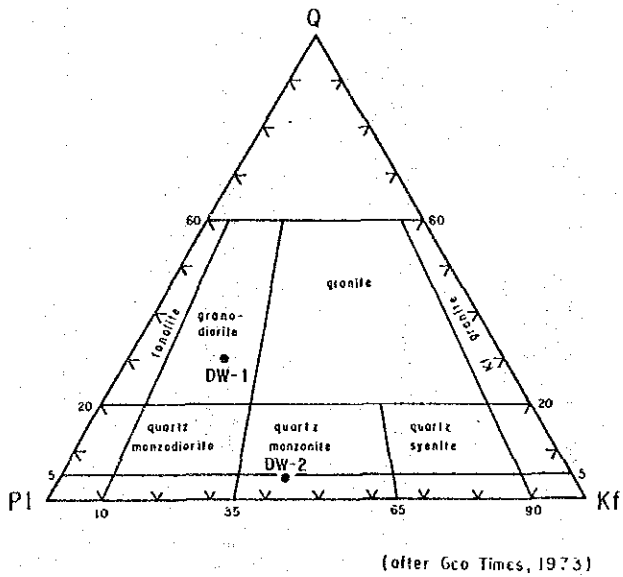

(after Geo Times, 1973)

Fig. 49 Normative Q-Kf-Pl Diagram of Intrusive Rocks in the Drill Holes

3–2–3 The Alteration of Peridotite

The wall rock alteration in the Mamute Mine area has been studied from a viewpoint of zonal arrangement in mineralization. Regarding the alteration of serpentinite, 4 types, i.e. tremolite type, talc type, chlorite type and weakly altered type can be devided by the distance from the intrusion of the adamellite porphyry. The tremolite type seems to be related with the mineralization and the others, to be related with the adamellite porphyry intrusion (WAKITA 1981).

As many drill holes intersected serpentinized peridotite, alteration studies for the cores from MJM-2, 4, 6 and 9 holes were carried out to delineate the center part of mineralizations.

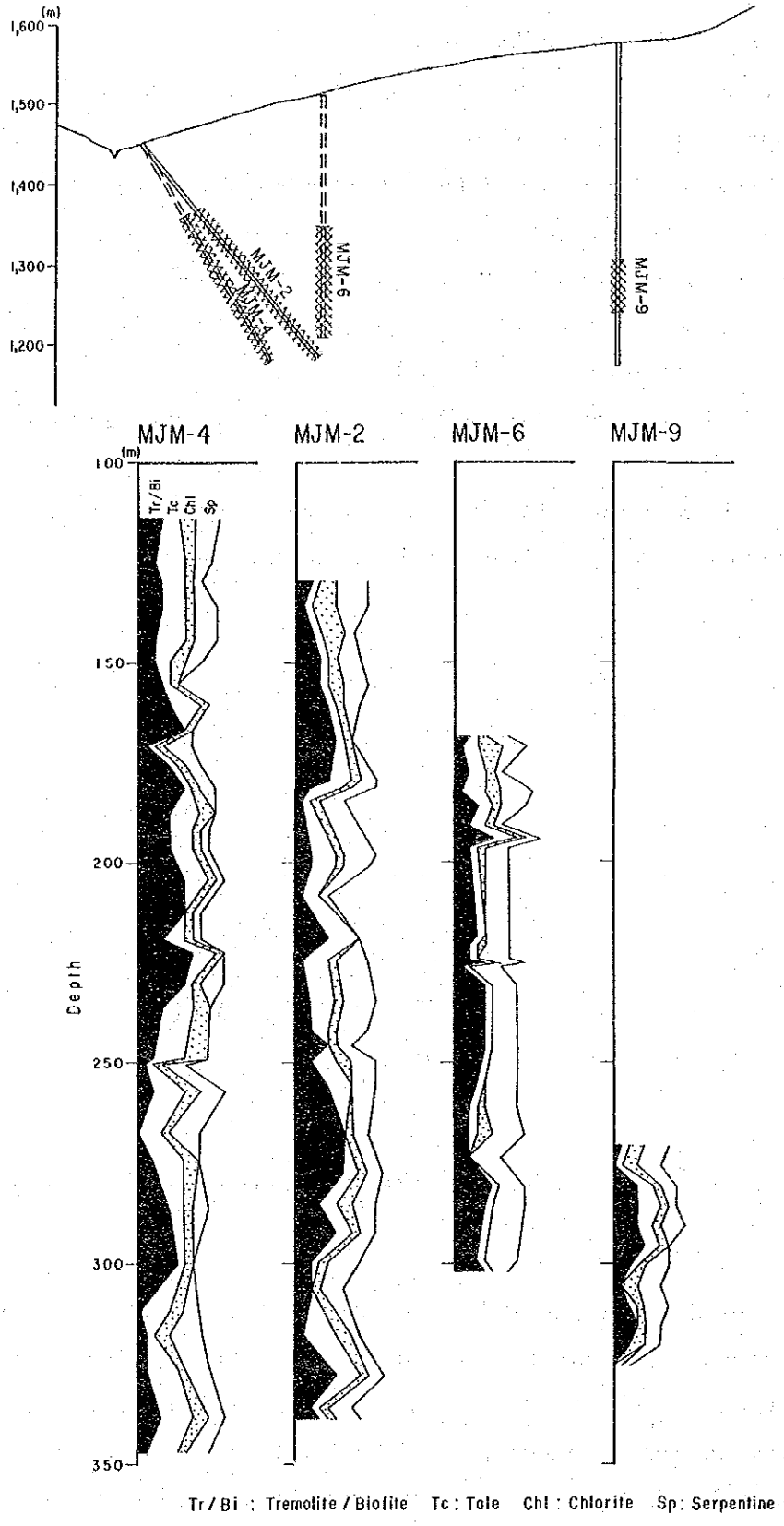

Fig. 50 Alteration Pattern of Serpentinized Peridotite

100 pcs of peridotite core samples taken from each hole at 5–10 m intervals were tested by X-ray diffractive analysis.

Fig. 50 shows intensities of four minerals assambrage (tremolite + biotite, talc, chlorite and serpentine) in each drilling hole. The followings may be discussed.

(1) Tremolite + biotite occurs in almost whole sections of 4 holes and tend to increase gradually as MJM-9 →6 →4 →2.

(2) The occurrences of talc are less amount in MJM-9 and 6 and become abundance toward MJM-4 and 2 holes.

(3) There are few difference of amounts in chlorite mineral among 4 holes.

(4) Serpentine is well observed in MJM-6 hole and decreases its intensity gradually as MJM-6 →4 →9 →2.

Besides of these, the more less amounts of anthophyllite were questionally detected in MJM-2 and 4 holes and olivine remains as original mineral in MJM-2 and 4 holes and a few in MJM-6 hole. It is summarized as follows:

Tremolite and talc alterations are intense in MJM-2 and 4 holes and weaken toward MJM-6 and 9 holes. However, chlorite and serpentine alterations are intense in MJM-6 and 4 holes and very weak in MJM-2 hole. Therefore, finally it is suggested that the hydrothermal alteration are to be strengthening from MJM-9 hole to MJM-2 hole.

3–2–4 Characteristics of the Pinosuk Gravels

As is evident from the geological profiles of this area, the Pinosuk Gravels widely covering the area between the Mamut Mine and the Bambangan Creek are proved to be much thicker than that was expected.

The drill hole of MJM-10 located in the upper stream of the Bambangan Creek deliniates that the base of the Gravels declines about 50° toward east from the creek area, and the thickness shows vertically 290 m to the surface. From the viewpoint of the topograph, the thickness increases presumably toward east and reaches to more than 450 m. However, the Gravels decrease its thickness toward south from the MJM-10 hole, with 270 m at MJM-9 hole and 161 m at MJM-6 hole. It is to say that the vertical shape of the Gravels shows a shape of bilge paralleling to the Bambangan Creek.

The characteristics of the Pinosuk Gravels in both vertical holes of MJM-6 and 9 are as follows;

(1) The Pinosuk Gravels may be divided into two parts, i.e., loose Gravels (0 m – about 50 m below surface) and solid Gravels, though their boundary changes gradually. The difference

between two characters may be due to compaction of dead load.

(2) As shown in Fig. 51, the kinds of gravels and gravel-matrix ratios are slightly different with the depth. The composition of the gravels at 0 m – 65 m depth of MJM-6 resembles those at 120 m – 200 m depth of MJM-9. If those of Pinosuk Gravels belong to the same horizon, it may be assumed that the bottom of gravels of MJM-9 is 60 m deeper than that of MJM-6 hole, which indicates eastward inclination of the gravels.

(3) Regarding the matrix, those between the loose and solid Gravels tend to be sandy and silty to muddy, respectively.

(4) The boulders and pebbles show angular to subangular in form. The boulder size occur abundantly in the loose Gravels and the pebble size increases in the lower part of solid Gravels.

(5) Regarding gravels-matrix ratio, gravels are rich in the loose Gravels and matrices are rich in the solid Gravels.

(6) In some gravels, composing the Pinosuk Gravels, such as gravels of adamellite porphyry, adamellite, microdiorite, hornfels and quartz, the pyrite and chalcopyrite can be observed in a shape of stringer or dissemination.

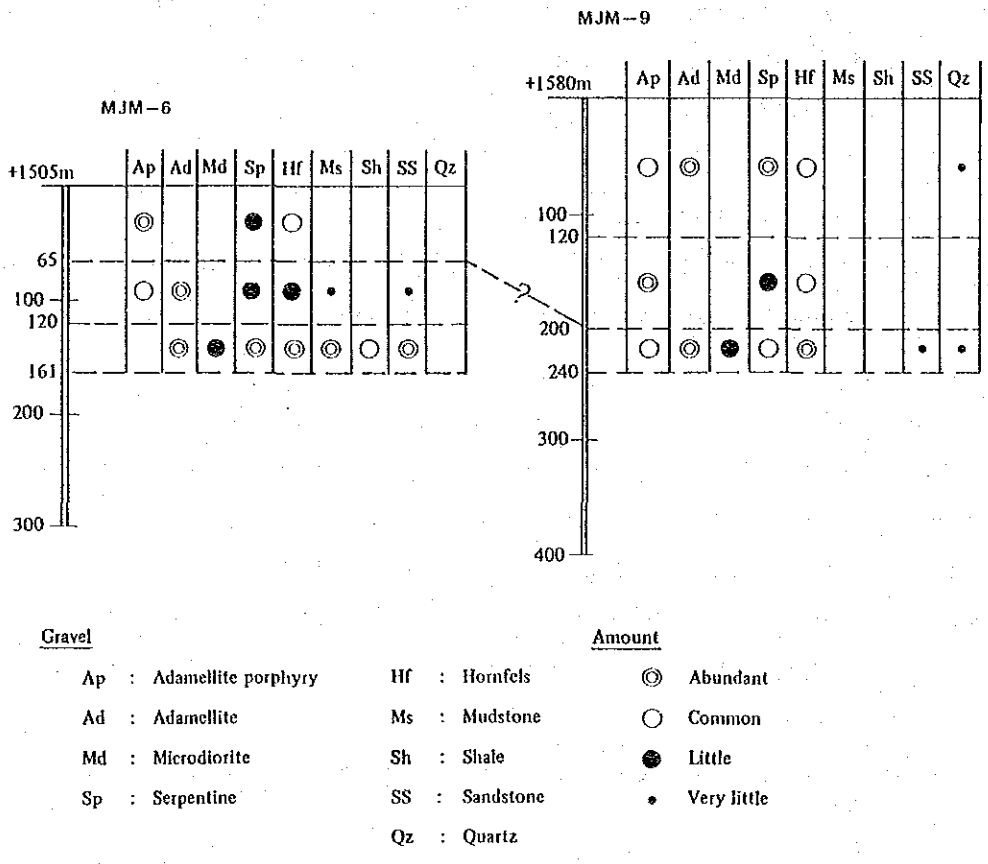

Fig. 51 Characteristics of Pinosuk Gravels at MJM–6 and –9 Holes

Chapter 4 Overall Discussion

As the Bambangan area is covered by Quaternary Pinosuk Gravels, a CSAMT survey was carried out in A area to select the potentiality of mineralization from the aspects of electrical resistivity structure and distribution causing by the intensity of resistivity underlying the Pinosuk Gravels.

As a result, the following 3 lower resistivity zones with the figures of lower than 100 Ωm were detected.

Table 11 Characteristics of CSAMT Anomalous Zones

Anomaly Distribution Zone		Characteristics	Mineralization
A-1	West of the Pit-site	* Resistivity of 50–70ohm-m is dominant. * The Pinosuk Formation around 50ohm-m shows a strong weathering.	50ohm-m detected in the lower zone of the Pinosuk Formation reflects the mineralization with argillization.
A-2	Center of the survey area	* Low resistivity zones are detected along the faults with different size. * Low resistivity less than 30ohm-m dominant. * No IP effect observed.	Low resistivity less than 30ohm-m detected here may be caused by clay and ground water filled in the fracture zone. Less possibility of existing mineralization.
A-3	North-western end of the survey area	A low resistivity was detected at the contact zone with a high resistivity zone. The resistivity around 30ohm-m is dominant.	The resistivity structure resembles the A-1 resistivity zone, suggesting the mineralization.

In A-1 resistivity zone, IP and SIP surveys were conducted to confirm existence of sulphide minerals and the aspect of resistivity zone. As a result, a structural line of resistivity with a direction of NW-SW system presumably occur in the center of the area and a clear IP anomalous zone with 30 – 40% FE was detected on the west of the Bambangan Creek. From the geology, the former structural line is considered to be a fault. The latter anomalies was confirmed by MJM-8 drill hole to be a dissemination zone of a porphyry copper mineralization associated with adamelite porphyry intrusion.

The shape of distribution of IP anomalies indicates that the mineralized zone extends along N-S direction with a westward dip.

The results of X-ray diffraction analysis for the peridotite smaples selected from 4 drill holes also suggests that the alteration relating to the mineralization becomes gradually stronger from the east to west (toward Bambangan Creek). The drilling survey, therefore, shall be recommended in the area including the locations of MJM-2, 4 and 8 holes.

It has been proved that the IP and SIP surveys are more effective as technique for the exploration of porphyry copper deposits in the area, so that the same method shall be recommended to apply for the area of A-3 resistivity zone, which shall be promising area for mineralization.

The A-3 zone is in the area of down stream from the Cu anomalies of stream sediments detected by both UNDP survey and Malaysian – West German survey, and having a weak altered zone, so it suggests high potentiality for copper mineralization.

The thickness of Pinosuk Gravels is rather more thicker than that was expected (maximum thickness is more than 450 m) in the area between Mamut mine site and Bambangan Creek.

There are some occurences of veinlet, and dessemination of pyrite bearing chalcopyrite in the boulder of Adamellite porphyry and Adamellite of Pinosuk Gravel. Therefore the geochemical copper anomalies, detected by UNDP Survey and OMRD Survey, are to be caused by this phenomena.

Judging from the results of IP and SIP surveys, no remarkable anomalies have been detected on the horizon of around 200 m depth from the surface, so that the potentiality of mineralization in the area seems to be rather lower.

PART Ⅲ B,b(MANKADAU) AREA

Chapter 1 Geology and Mineralization

1–1 Geology

1–1–1 *Sedimentary Rocks*

The sedimentary rocks and lavas that underlie this area appear to be correlated with the Trusmadi Formation judging from the characteristics of rock facies. However, the relationship between the lower part of the Trusmadi Formation and upper part of the Chert-Spilite Formation is a lateral facies change and the basalt, occurs in both, which will be mentioned latter. Thin layers of chert are also observed in the sedimentary facies. Therefore sedimentary rock facies might be correlated with the Chert-Spilite Formation; however no further supporting evidence was available.

Geological map and schematic columnar section are shown in Fig. 7 and Fig. 8.

Each of the rock facies is described as follows.

(1) Sandstone

The sandstone is grey to dark grey, medium to fine grained, hard and compact, and alternates rhythmically with dark grey siltstone layers in some parts of the Area, with pyrite inpregnated nodule (1 cm in diameter) and are often observed in large ball-shaped sandstone nodule. Sole marks are also observed on the surface of weathered sedimentary rock in the middle of Lingangaa creek. The sandstone facies gradually changes into siliceous sandstone in some parts, but its distribution is irregular. No fossil is found in the Area.

The results of microscopic study of the representative samples are as follows;

Y–49 Medium grained sandstone

Grains : quartz > chert fragments, plagioclase, calcite > K-feldspar, zircon, opaque minerals

Characteristics : mainly consists of quartz with a number of chert fragments, plagioclase and are arkosic. Sorting and grading are poor. Shape of grains shows subangular to subrounded with diameters of up to 0.4 mm. The matrix is composed mainly of pelitic facies containing fine grained quartz, K-feldspar, plagioclase and calcite. Secondary minerals are calcite, sericite and chlorite.

F–01 Siliceous sandstone

Grains : quartz > chert fragments > K-feldspar, plagioclase, hornblende

Characteristics : Quartz grains are abundant and irregularly shaped with a mozaic texture. The grain size is 0.3 mm±. The rock fragments present are chert. Matrix are less abundant, con-

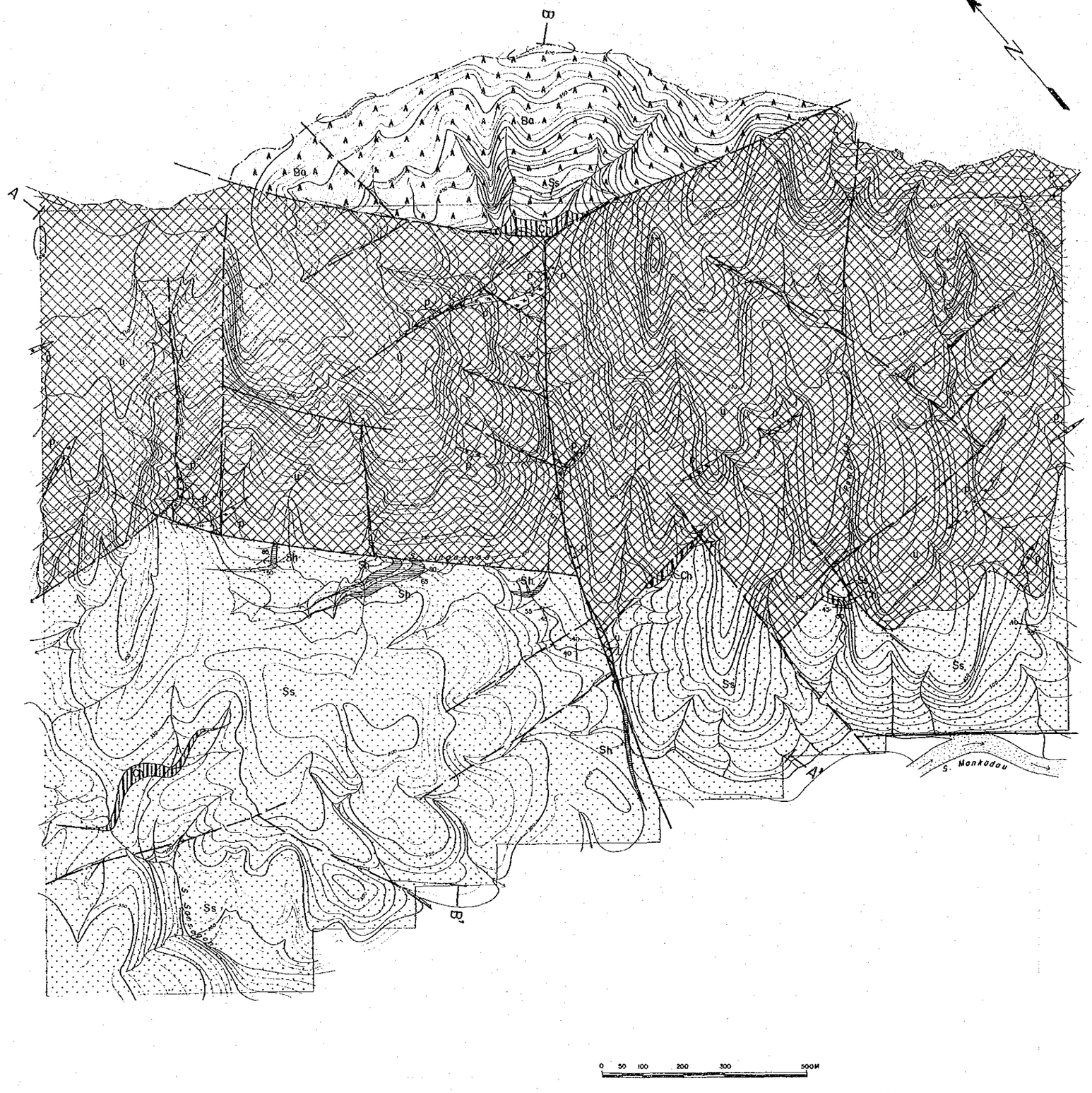

LEGEND

Trusmadi Formation

Ss sandstone
Ch chert
Sh shale
Ba basalt

Intrusive Rocks

p pegmatite
u ultrabasic rock

Fault (certain)
Fault (inferred)
70/30 Strike and dip
A—A' Geological Profile line

Fig. 52 Geological Map of "b" Area

sisting of micro-crystalline and opaque minerals. The secondary minerals are chlorite and quartz.

2) Shale

The shale is characterized by reddish brown coloured, lamellar and thin layers, and locally it shows rhythmic alternation with sandstone. The shale is rather silty and softer than the sandstone. The shale, distributed in upper Lingangaa creek shows well developed lamella. It is recognized as the result of mechanical deformations by faulting. The shale facies distributes throughout the Area, (however, it is rare that the distribution is mappable).

Thin layers of chert are distributed in the central and south-western part of sandstone facies of the Area, rarely intercalated in basalt lavas, which will be described later. Its occurrences are rather lenticular in shape. The rock facies is greyish brown, hard, well-bedded, with quartz stringers (less than 1 cm wide) in some part of the area.

Stratigraphic horizon; The sedimentary rocks in the area are in fault contact with the ultrabasic rocks. No fossil is found. Therefore it is very hard to correlate the horizon however it is similar to an eugeosynclinal flysch sediments or rather molasse.

3) Basalt

Distribution and thickness; It is distributed along the ridge of northeastern part of the Area. The thickness is over 300 metres.

Rock facies; It consits of basalt and andesitic lavas intercalated with sandstone and thin chert layers. It shows many pillow structures, with little hyaloclastite. It also shows amygdaloidal structure, strongly brecciated, especially along the boundary of peridotite.

The results of microscopic study of the representative samples are as follows;

S–22 Olivine basalt

Texture : intersertal

Phenocrysts : plagioclase ≫ augite, olivine

Characteristics : The Phenocrysts consist of plagioclase with minor amount of augite and olivine. The plagioclase phenocryst are euhedral to subhedral and up to 2 mm in length. The augite is subhedral up to 0.5 mm in length and is generally altered to epidote whereas the olivine is altered to serpentine and iron minerals. The groundmass consists of fine grained plagioclase laths, glass, and opaque minerals. Secondary minerals are zeolite, calcite, epidote and iron minerals. Calcite occurs as veinlets.

Y–23 Olivine basalt

Texture : intersertal, amygdaloidal

Phenocrysts : plagioclase ≫ hypersthene, olivine

Characteristics : It shows intersertal and partially amygdaloidal texture. It is strongly cal-

citized. Phenocrysts of plagioclase are subhedral with the size of 1 to 3 mm. The colored minerals are hypersthene and olivine, however the olivine is completely replaced by calcite, so it was recognized from pseudomorph of olivine. The matrix mainly consists of plagioclase laths with minor glass. The altered minerals are calcite, actionolite, zeolite and hematite. This specimen is strongly brecciated, and filled by iron and/or manganese minerals and calcite in some places.

The sandstone and chert are intercalated with these basalt lavas. The sandstone is grey, massive without stratification, containing ball of nodule whose size is 1 m in diameter. The chert is greyish brown, hard and well-bedded. These characters are similar to sandstone in sedimentary rocks. The basalt has the strong calcitization in overall area. In the gully around this area, there are some amount of pale brown calcite as secondary origin.

Stratigraphic horizon; The horizon of these lavas are not clear, because they occur in fault contact with the peridotite. However, judging from the rock facies it is correlated with the spilite of Trusmadi Formation. It appears to overlie the sandstone of sedimentary rock facies.

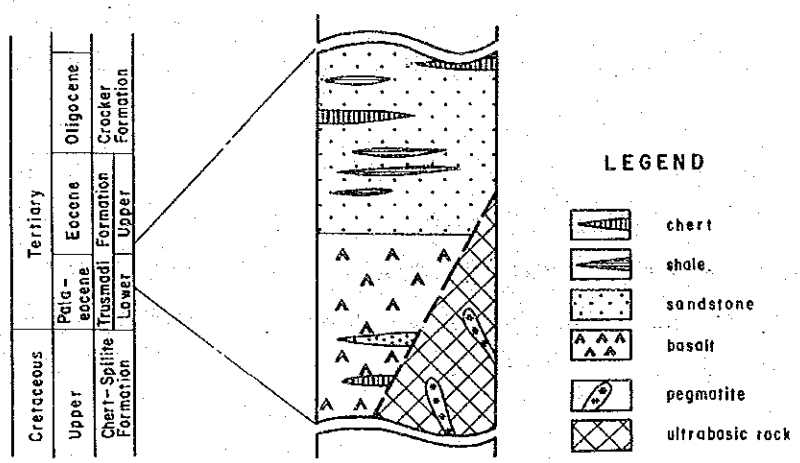

note) Intrusion and emplacement of ultrabasic rock are supposed to be in Cretaceous age and early Miocene age respectively.

Fig. 53 Generalized Stratigraphic Section of "b" Area

1–1–2 Intrusive Rocks

The intrusive rocks found in the area include peridotite and pegmatite.

(1) Peridotite

Distribution; These rocks are distributed widely in the central part of the area trending northwest to southeast.

Rock facies; The rock is rather hard and resistant to weathering with cliff-like exposure. The color is melanocratic and glossy. The rock is composed of harzburgite with layered dunite. Both rocks are affected by strong serpentinization and brecciation in part of the Area with various degrees of irregular brecciation. The occurrences of talc and magnesite stringers (5 cm –) are also common. The granular materials (diameter 1 to 3 cm) in the creek are the product of iron-rich laterization, forming a crust derived from the process of weathering.

The characteristic of representative sample under microscopic study are described as follows;

S–31 Harzburgite

Texture : equigranular

Minerals : olivine > orthpyroxene, opague minerals

Characteristics : strong serpentinization

Observing the pseudomorph under parallel nicol, the serpentine occurs as stringers in some part forming mesh-structure. Orthopyroxene (seems to be enstatite) has altered to actinolite. Other secondary minerals are a small amount of sericite and opaque iron minerals.

In lower Lingangaa creek and Pompudum creek, the dark bluish grey and massive peridotite with strong calcitization is distributed along fault zone.

Y–28 Harzburgite

Texture : equigranular

Minerals : olivine > orthopyroxene > chromite, opague minerals

Characteristics : very strong calcitization, olivine and orthopyroxene also completely altered to calcite (pseudomorphs identified under parallel nicol). Minor amount of chromite is found. The secondary minerals are zeolite and irregular shaped quartz.

This rock is in fault contact with sandstones and basalt lavas on the south side and north side respectively.

The period of intrusion is Cretaceous and its emplacement is assumed to be in early Miocene.

(2)

Distribution; distribute within the peridotite facies. The pegmatite dykes, trending E-W have a maximum length of 200 m; The width of dykes varies with the maximum of about 30 m. The pegmatite occurs along faults in the peridotite.

Rock facies; Leucocratic. Composed of quartz and plagioclase with minor amphibole and mica. The rock is very hard and resistant to weathering. The crystals of quartz and plagioclase show euhedral to subhedral shapes, and are commonly a few centimetres in length (rarely over

Table 12 Chemical Composition of Ultrabasic Rock

		New sample		Previous sample		
Serial No.		1	2	3	4	5
Sample No.		S–31	Y–43	–	–	–
Location		B07–10	B37–05	Mamut	Mamut	Mamut
Rock Name		harzburgite	harzburgite	serpentinite	serpentinite	peridotite
Chemical Composition	SiO_2 %	43.65	42.86	42.90	40.43	40.94
	TiO_2	0.04	0.05	0.05	0.14	0.14
	Al_2O_3	1.11	1.27	3.08	4.99	3.97
	Fe_2O_3	4.67	4.14	7.25	6.21	3.87
	FeO	2.24	2.56	2.43	1.85	4.28
	MnO	0.09	0.11	0.14	0.10	0.12
	MgO	35.43	35.89	30.83	34.48	36.28
	CaO	0.09	0.11	4.07	3.02	2.63
	Na_2O	0.03	0.04	0.11	0.23	0.08
	K_2O	0.05	0.07	0.63	1.00	0.03
	P_2O_5	0.01	0.01	0.18	0.18	0.02
	BaO	0.06	0.12	–	–	–
	Lgn. loss	13.07	13.36	7.85	8.18	7.51
	Total	100.54	100.59	99.54	100.84	99.87
100xMgO/MgO+FeO*		89.08	89.03	84.40	88.14	85.77

note) No.3: A–16(186m), analyzed by O.M.R.D. Sabah Bhd.
No.4: E'–14(159m), analyzed by O.M.R.D. Sabah Bhd.
No.5: J6431, from Jacobson(1970)

Table 13 Chemical Composition and CIPW Norm of Basalt

Sample No.		S–21	T–32
Location		160m north of B30–01	250m north of B36–01
Rock Name		basalt	basalt
Chemical Composition	SiO_2 %	50.23	54.93
	TiO_2	0.84	1.05
	Al_2O_3	15.17	17.34
	Fe_2O_3	3.11	8.58
	FeO	4.33	0.34
	MnO	0.15	0.14
	MgO	6.04	1.20
	CaO	11.77	7.70
	Na_2O	2.99	5.61
	K_2O	0.77	0.35
	P_2O_5	0.18	0.01
	BaO	0.13	0.09
	Ign. loss	5.31	3.60
	TOTAL	100.84	100.94

Sample No.			S–21	T–32
C.I.P.W. Normative Minerals	$Q^{wt\%}$		0.98	6.34
	c		0.00	0.00
	or		4.55	2.07
	ab		25.30	47.47
	an		25.70	21.10
	ne		0.00	0.00
	wo		0.00	2.98
	di	wo	13.26	3.46
		en	9.42	2.99
		fs	2.68	0.00
	hy	en	5.62	0.00
		fs	1.60	0.00
	ol	fo	0.00	0.00
		fa	0.00	0.00
	mt		4.51	0.00
	ht		0.00	8.58
	il		1.60	1.02
	tn		0.00	1.26
	ru		0.00	0.00
	ap		0.42	0.02
	TOTAL		95.63	97.28

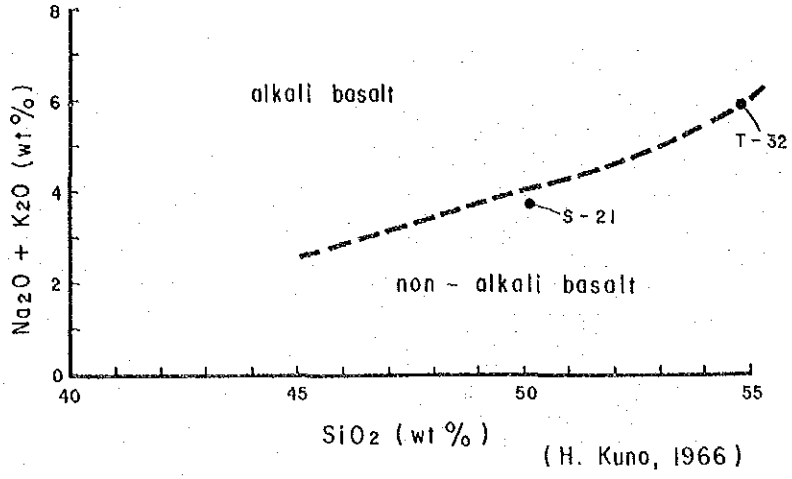

Fig. 54 $Na_2O + K_2O - SiO_2$ Diagram of Basalt

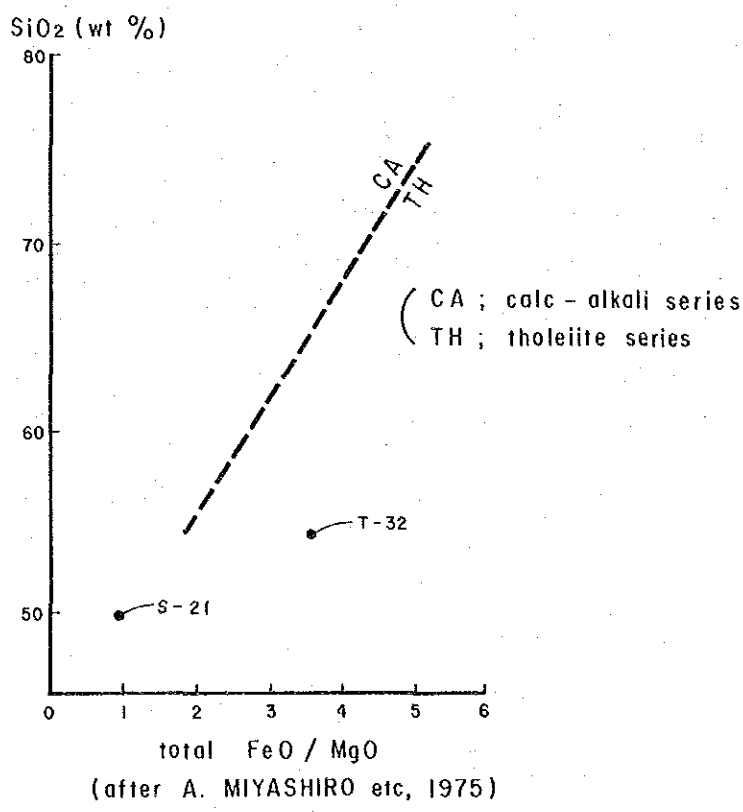

Fig. 55 SiO_2 – total Fe/MgO Diagram of Basalt

10cm). The amphibole and mica are also euhedral to subhedral, but of less abundance and localized.

The characteristics of pegmatite under microscopic study are as follows;

T–20 Pegmatite

Texture : equigranular, holocrystalline

Minerals : plagioclase ≫ quartz, hornblende

Characteristics : Mainly albite-twinned plagioclase with minor quartz and hornblende. No mica has been found in this sample. The plagioclase are few centimetres in size, and the hornblende are 0.5 to 2.5 cm long, with a equigranular texture. The bending albite twin in plagioclase are also found, with small streak developed partially. Minor amount of pumpellite are also found as secondary mineral.

1–1–3 Characteristic of Intrusive Rocks

The peridotite and two basalt samples were tested. The chemical analytical values and norms of these samples are shown in Table 4 and 5 respectively.

(1) Peridotite

Table 4 shows the chemical results together with the results from previous work. The values of 100 x MgO/(MgO + FeO) are also included in the table.

The two samples contain 43% of SiO_2, have similar values of other elements. The value of 100 x MgO/(MgO + total FeO) is 87 in both samples; therefore it falls within the category of Alpine-type ultrabasic rock.

The composition of peridotite in the b area is almost same as those of serpentinite or peridotite collected around the area of Mamut mine.

(2) Basalt

The values of SiO_2 of two samples are 50.23% and 54.93% respectively and fall within the composition of basalt to andesite.

The diagram of $SiO_2 - Na_2O + K_2O$ (Fig. 54) shows that these two samples plot near the boundary between Alkalic-basalt and non Alkalic-basalt. It is clear that these samples are of the tholeiite series from SiO_2 – total FeO/MgO diagram as shown in Fig. 55.

The rock originally was non Alkalic-basalt, however the addition of Na as a result of spilitization ($CaAl_2Si_2O_8 + Na_2CO_3 + 4SiO_2 \rightleftharpoons 2NaAlSi_3O_8 + CaCO_3$) makes the rock alkalic.

1–1–4 Structure

Faulting and folding are rather predominant in the Area. The predominant fault system,

trending E-W is well developed; NW-SE and NE-SW systems which cross obliquely to E-W faults are also developed (Fig. 56).

The fault patterns in the Area can be divided into four systems. The first is NNW-SSE and NE-SW systems in sedimentary rock and/or peridotite. The periods of fauting are probably as follows;

The Faulting in sedimentary rocks took place from early Neogene to middle Neogene, and those in peridotite rock in Miocene.

The second and third are E-W, NW-SE systems and N-S system respectively. The distribution of peridotite is controlled by these fault systems. The faults have high to vertical angles. The same fault systems also occur in sedimentary rocks. The fault system of E-W and NW-SE directions are considered as having formed during the same period.

The latest faults are the E-W faults which occur boundary between the ultrabasic rock and basalt. This direction is the same as E-W system mentioned earlier; however it shows remarkable dislocations.

The pegmatite dykes intruded into the peridotite in an E-W direction parallel to the fault system. The E-W faults presumably provided channel ways for the pegmatite to intrude into the peridotite.

The rose-diagram in Fig. 57 shows the total length and frequency of faults and pegmatite dykes. Comparing the two diagrams, the E-W direction stands out.

Although the anticlinal axes were not determined in the field, the anticlinal structures, appear to trend in the NW-SW direction, the same as the distribution of peridotite. The direction of deposition of sedimentary rocks is at an oblique angle with the direction of anticlinal axis.

1–2 Mineralization

The geological survey has delineated:

(1) the occurrences and characteristics of the floats of massive copper-rich sulfide ore in the middle of Lingangaa creek and (2) the occurrences and characteristics of the floats of massive chromite ore in the upper northwestern part of the area.

1–2–1 Alteration

This includes spilitization of basalt and serpentinization in the peridotite. In addition lateritization is also found.

The distribution of alteration zones in the area is shown in Fig. 58.

Spilitization is commonly observed in basalt which occurs in the northeastern part of the

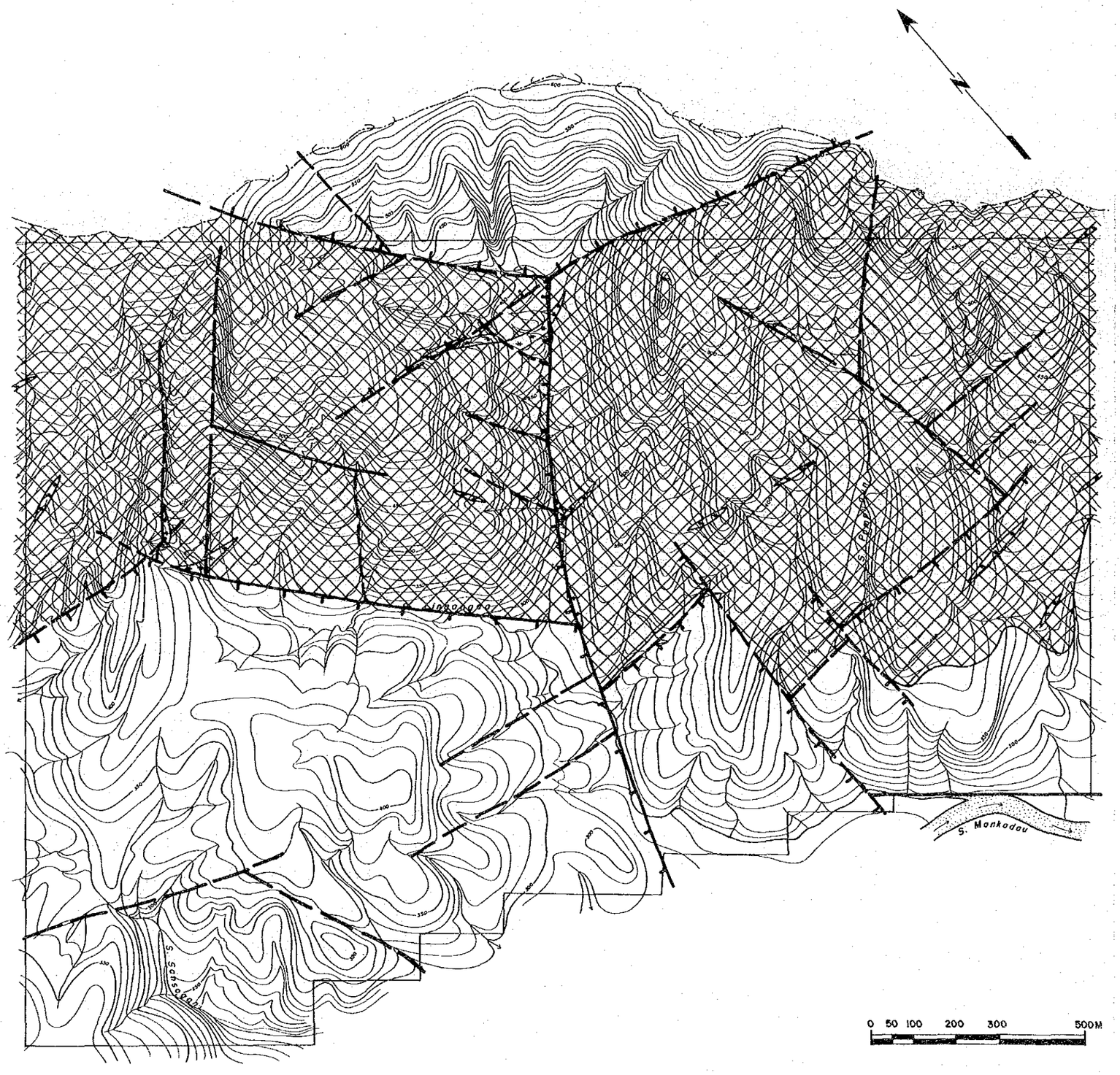

LEGEND

down — fault (certain)

down — fault (inferred)

Intrusives

pegmatite

urtrabasic rock

Fig. 56 Structural Map of "b" Area

(Faults)

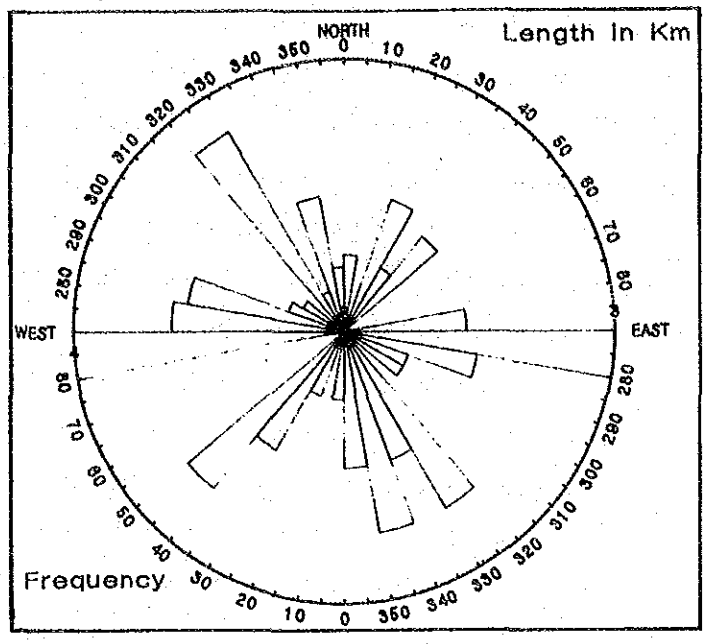

(Pegmatite)

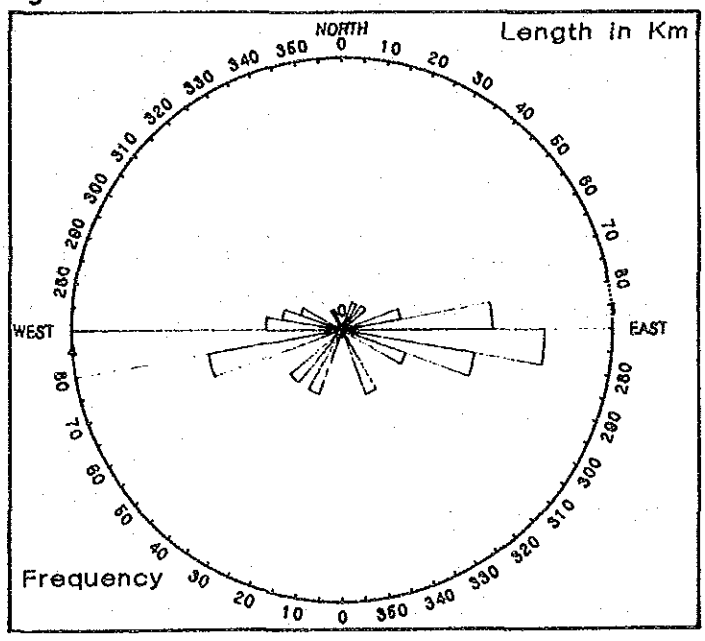

Fig. 57 Rose Diagram of Structural Elements in "b" Area

area. The primary rock facies is that of tholeiite series which belongs to non-alkali basalt. The calcareous plagioclase are altered to albite by the spilitic reaction.

After the alteration, the material of secondary sedimentation by calcitization is found in basalt lavas. Under the microscope, it is observed that the serpentinized olivine, epidotized pyroxene, and zeolite, calcite chlorite occur as secondary minerals.

Serpentinization is common in peridotite which occurs in the northeastern part of the Area, trending NW-SE. Serpentine which replaces olivine, is mainly antigorite which was detected by X-ray diffractive methods. Talc also occurs near the fault zone.

Red-colored soil is found in several areas underlain by peridotite and may be the result of lateritization (including either ferrification or subfication). Laterization also occurs in basalt. This distribution red-coloured soils is shown in Fig. 13. A wide distribution occurs in the northern part of the area where peridotite occurs. The lateritic soil consists mainly of iron-aluminium hydro-oxides and are identified by X-ray diffraction as limonite, geothite and magnetite. The lateritic crust in same category as mentioned above are also found in the same area. This is described as an oolitic material forming a crust with banded limonite. The central part of oolite shows concentric structures of irregularly accumulating muddy and dusty materials, and limonitic mixture. The concentric structures develop from nuclei of sand or magnetite grains.

In addition, argillized soil which is mainly found over sedimentary rocks is also present. Its occurrence as brown soil is limited to along fault zone.

1–2–2 Mineralization

(1) Massive sulfide ore

Floats of massive sulfide ore are found in Lingangaa creek along the fault contact between sedimentary and peridotite. The distribution of such floats is only confined to the Lingangaa creek. (Fig. 58 and Fig. 59)

The ore minerals are chalcocite, bornite, covellite, chalcopyrite and pyrite. This assemblage is varied in some parts;

chalcocite – bornite-covellite-chalcopyrite,

chalcopyrite-pyrite,

and mixed assemblages of the two mentioned above. The gangue mineral is ferruginous quartz. The distribution of these minerals in floats is irregular but massive. However the assemblage of chalcopyrite-bornite shows banded structure in some parts. The ferruginous quartz is reddish brown in color and malachite streaks are also observed.

The result of chemical analysis of the ore is shown on Table 14. The samples Y–50(1),

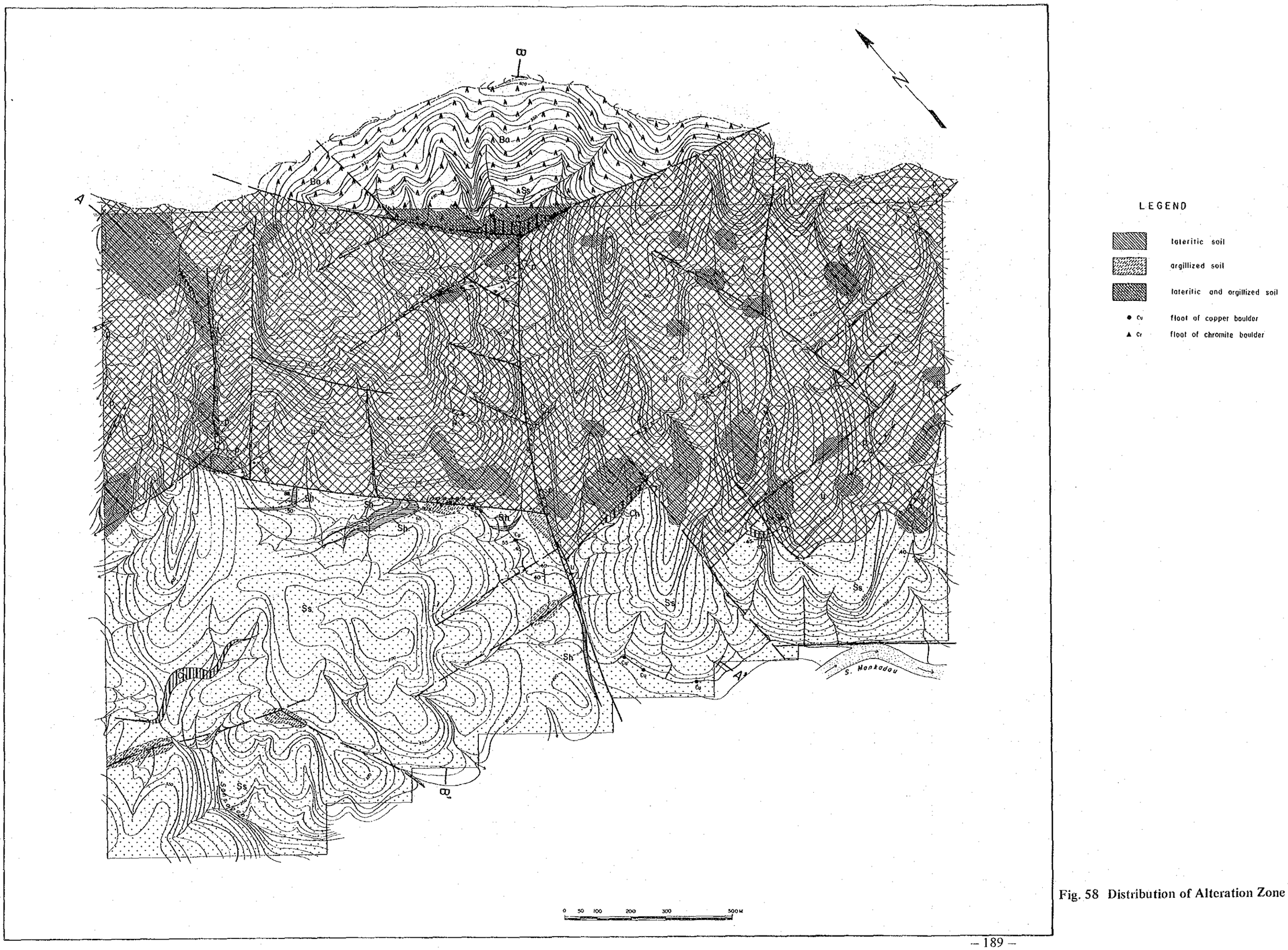

Fig. 58 Distribution of Alteration Zone in "b" Area

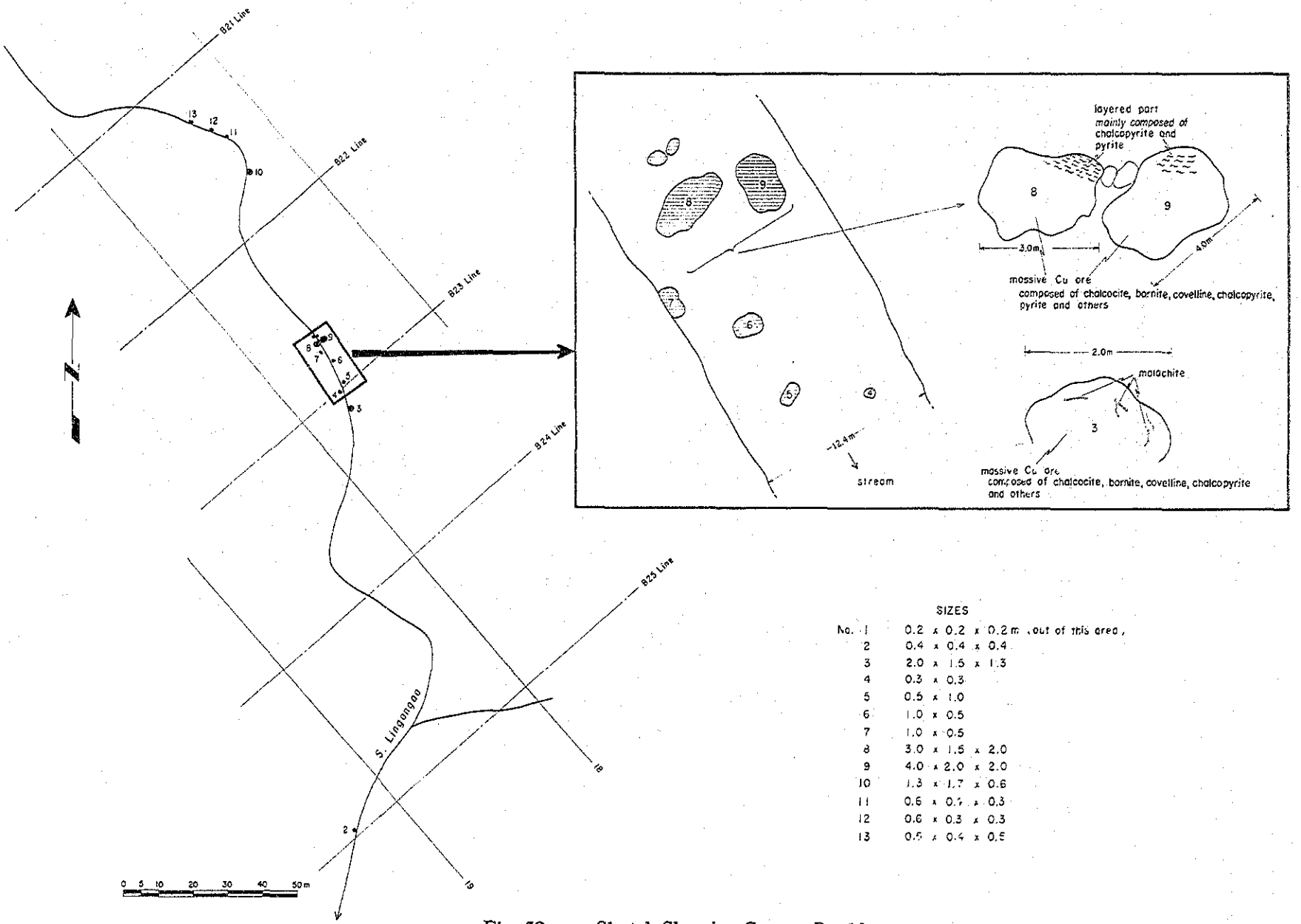

SIZES

No. 1	0.2 x 0.2 x 0.2 m (out of this area)
2	0.4 x 0.4 x 0.4
3	2.0 x 1.5 x 1.3
4	0.3 x 0.3
5	0.5 x 1.0
6	1.0 x 0.5
7	1.0 x 0.5
8	3.0 x 1.5 x 2.0
9	4.0 x 2.0 x 2.0
10	1.3 x 1.7 x 0.6
11	0.6 x 0.4 x 0.3
12	0.6 x 0.3 x 0.3
13	0.5 x 0.4 x 0.5

Fig. 59 Sketch Showing Copper Boulder

Y-50(2) and Y-51 are chalcocite-bornite massive ore. Y-31 is a chalcopyrite-pyrite banded ore. The former group shows higher copper values than the latter. Both lead and zinc values are very low compared with copper.

Table 14 Chemical Composition of Copper Boulder

Sample No.	Location	Specimen	Au(g/t)	Cu(%)	Pb(%)	Zn(%)	Mo(%)	Hg(%)
Y-50(1)	B23-19	massive sulfide ore	1.16	48.28	0.03	0.02	0.034	<0.001
Y-50(2)	B23-19	massive sulfide ore	31.00	41.12	0.25	0.19	0.060	<0.001
Y-31	B23-19	massive sulfide ore	1.85	24.61	0.08	0.14	0.012	<0.001
Y-51	B23-19	massive sulfide ore	1.37	64.88	0.10	0.02	0.096	<0.001

The distribution of floats described above has been reported from earlier investigation which included some chemical analyses. For example, A. Soriano Y. Cia's figure (1962) was 45.2% of copper and Lim Peng Siong's figure (1982) was 38.0% and 34.0%. The gold contents are also very high, 1 to 2 g/t. Nevertheless 31 g/t of gold was detected for Y-50(2). However all specimens were collected individually and no gold grains were observed under the microscope. Therefore the occurrence of gold could be localized.

The result of microscopic observation is as follows.

Y-50 Cupriferous secondary sulfide ore

Ore minerals : chalcocite > covellite > bornite > pyrite

Characteristics : Among these ore minerals, the first three occur in various ratios; bornite is abundant in some parts. However the others are abundant in chalcocite and bornite. No chalcopyrite has been found.

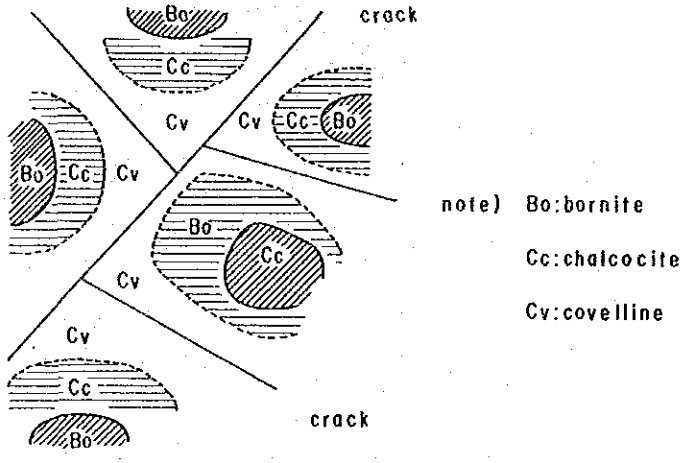

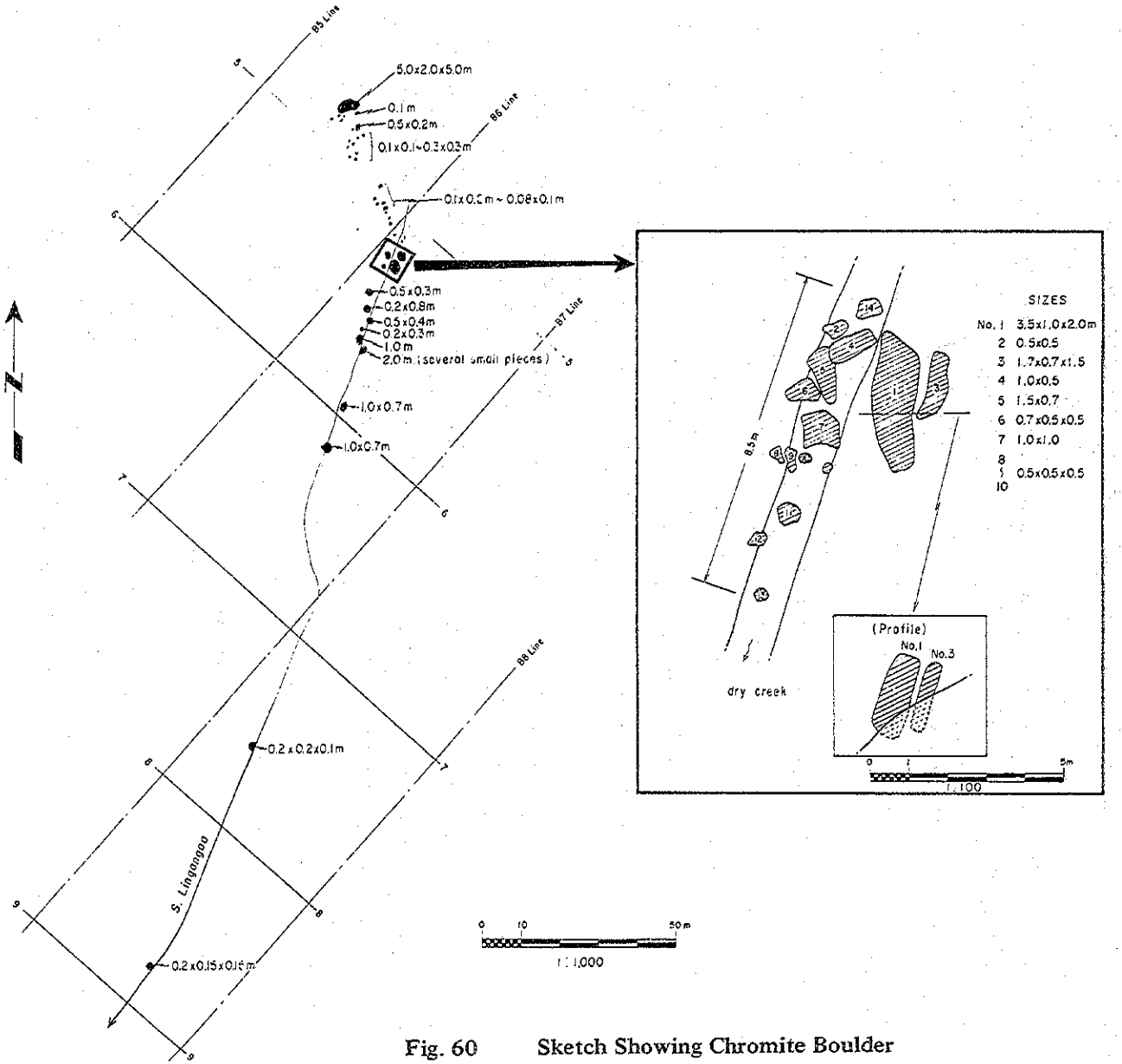

Fig. 60 Sketch Showing Chromite Boulder

From this observation, it is noted that the primary bornite or pyrite has been replaced by covellite and chalcocite.

In this process the pyrite has been replaced by secondary copper minerals, therefore their crystal shapes have been altered. However cubic crystals are also noted and their sizes vary from 0.05 to 0.2 mm. This phenomenon shows that the replacement of pyrite is rather weaker than the replacement of chalcopyrite. Pressumably the original mineral assemblage was pyrite-chalcopyrite or pyrite-bornite.

Y–31 Cupriferous secondary sulfide ore

Ore minerals : chalcopyrite > pyrite > covellite

Characteristics : Very few bornite and unidentified very fine ore mineral.

Yellow part of specimen consists mainly of chalcopyrite pyrite, and grey part mainly chalcopyrite-covellite assemblage. Euhedral pyrite has been associated. Remarkably the texture is very fine felted. The size of pyrite crystals are under 0.01 mm in the assemblage of chalcopyrite-pyrite, and 0.01 mm± in the assemblage of chalcopyrite-pyrite-covellite. The covellite commonly is 1 to 3 mm, and chalcopyrite is presumably very fine from its paragenesis with pyrite and covellite.

Pyrite also forms colloform layers. Its shape is mainly pellet-shape with concentric-shape in some part (0.01 mm of each grain size).

Gangue minerals, mainly ferruginous quartz is found in Lingangaa creek and Pompudum creek, and all occur as floats. No outcrops have been found in this survey. However, the interesting point of this occurrence is that they are found at the boundary between sedimentary rocks and peridotite. The floats of ferruginous quartz boulders contain less amount of sulfide minerals.

The results of microscopic observation are as follows;

Y–27 Ferruginous quartz (Iron oxide)

Ore Minerals : hematite

Characteristics : Red part is composed of ferruginous quartz with quartz stringer. Quartz stringer has minor amount of hematite which formed colloform texture at the edge with botryoidal quartz. Ferruginous quartz hematite shows fish scale-like texture 0.04 to 0.01 mm long, and 0.002 to 0.004 mm wide. At the boundary between the ferruginous quartz and colloform texture are found quartz stringer; this means the quartz stringer occurs after ferruginous quartz.

Y–40 Ferruginous quartz (Iron oxide)

Ore minerals : hematite, pyrite

Characteristics : Very small amount of hematite with pyrite-like minerals dispersed in

quartz. Red colored part is assumed to be cryptocrystalline hematite. Visible hematite shows micro fish scale-like feature of 3μ in length and 5μ in width.

Data from previous and present surveys have contributed to a clearer picture of the occurrences and characteristics of floats of massive sulphide ore:

The distribution is only limited to Lingangaa creek.

High copper content in the ore is due to secondary enrichment reaction. The assemblage of primary ore minerals is recognized as pyrite-chalcopyrite and/or pyrite-bornite.

Banded structures are present in parts of the sulfide ore and that the ferruginous quartz occur as a gangue mineral.

Ferruginous quartz is distributed not only in Lingangaa creek but also in Pompudum creek: however it is limited only to the area of the boundary between sedimentary rocks and peridotite.

Ferruginous quartz contains minor sulfide minerals.

No sulfide mineral is found in peridotite.

(2) Chrome ore deposit

Floats of chrome ore were newly found in the survey. It is distributed in the uppermost part of the main Lingangaa creek. The floats of chromite are distributed in areas occupied by peridotite. It extends for more than 200 metres in N-S direction along the creek, with boulders as large as 5 x 2 x 5 m. The distribution is shown in Fig. 58 and Fig. 60.

The chromite ore is black colored, massive, hard and compact, with streaks (1 mm± in width) filled by pure green colored chlorite. Ore mineral is only chromite. Common gangue minerals are serpentine and chlorite. The host rock of this ore deposit is dunite; however it was not observed in either field survey or microscopic study. Nevertheless the chromite ore deposits in Sabah commonly occur in dunite host rock even though in the present survey the floats of ore deposit occur within an area occupied by harzburgite. Another occurrence of chromite ore deposit near the Area has been reported in Paranchangan area, 4 km southeast of the survey area, and its occurrence is very similar to this area, where lateritic red soil is found in the surroundings of the floats.

The results of microscopic study of the representative samples are as follows;

Y–52(1) Chromite ore (polished section)

Ore mineral : chromite

Characteristics : Chromite crystals with diameters of 1 to 3 mm; has many cleavages and fissures forming a network. It shows brecciated textured and in some parts, it is of finer grained size.

Presumably it is the evidence of mylonitization. The chromite mineral belongs to the spinel group; however study on the internal texture of crystal could not confirm the cubic crystal system of chromite.

Y-52 Chromite ore (thin section)

Minerals : chromite, serpentine, chlorite and actinolite

Characteristics : Chromite shows euhedral to subhedral shape; however many cleavages and fissures are irregularly developed by mylonitization. Serpentine is found in cleavages and fissures. Color of chromite is reddish brown to dark brown with high reflective index. Chlorite stringers cut all these minerals.

The results of chemical composition for these chromite specimens are shown in Table 15. The result shows that the specimens contain Cr_2O_3 of about 30 w% and belong to Picotite. The content of Ni and Co is also very high.

A point of interest is that these specimens are similar in character and chemical composition to the chromite ore which are found in Paranchangan area.

Table 15 Chemical Composition of Chromite Boulder

Sample No.	Location	Specimen	Cr_2O_3(%)	Total FeO(%)	SiO_2(%)	Al_2O_3(%)	MgO(%)	Ni(ppm)	Co(ppm)
Y-52(1)	B06-05	chromite ore	32.66	13.11	6.13	22.87	17.19	1,809	174
Y-52(2)	B06-05	chromite ore	31.28	12.00	7.84	23.07	16.90	1,709	160
T-34	B05-05	chromite ore	29.73	11.29	10.79	19.85	15.63	1,629	156

CHAPTER 2 GEOCHEMICAL SURVEY (SOIL)

2–1 Field Procedure

Geochemical sampling was made in a grid system of 50 x 50 meters (grid sampling of 50m x 50 m). The location of sampling was determined by handy survey referring to the existing 1 : 50,000 sclae topographical map. Fig. 61 shows the location of samples. The samples were collected only from B layer, and attention was payed not to be contaminated by soil of A and C layers, especially by humus soil on the surface.

The collected samples were dried in natural atmosphere, and put through a sieve to obtain silty soil under 80 mesh, which were provided for chemical analysis. The number of samples collected were 1,861 for each "b" Area and "c" Area.

The following sample number was used, for example, to make clear the sample localities.

B 25 – 31 . . . . . number of sample on survey line

. . . . . number of survey line with 50 meters spacing

. . . . . name of survey area

2–2 Laboratory Procedure

The samples prepared at the site were promptly sent to the Geological Survey of Malaysia, Sabah and chemically analyzed by atomic absorption method. The samples were analyzed for five components such as Au, Cu, Pb, Zn and Mo. Among these, Au analysis was made for selected samples.

The detection limit was 0.03 ppm in Au, and 1 ppm in Cu, Pb, Zn and Mo.

2–3 Data Treatment

2–3–1 Simple Statistical Analysis

It was estimated that the background of each element analyzed would be different each other because of different chemical composition for each rock facies of the rocks distributed in the target area. Therefore, histograms were produced to examine the mode of distribution of the assay values for each element (Fig. 62). As a result, it became clear that the distribution of assay values show a normal distribution on the histogram, resulting from classification of the rock facies.

Furthermore, (cumulative frequency curves) were produced to give threshold for extra-action of anomalous values (Fig. 63). These are the plots of reverse cumulative frequency on the log-probability curve, which were calculated from histograms by accumulation of

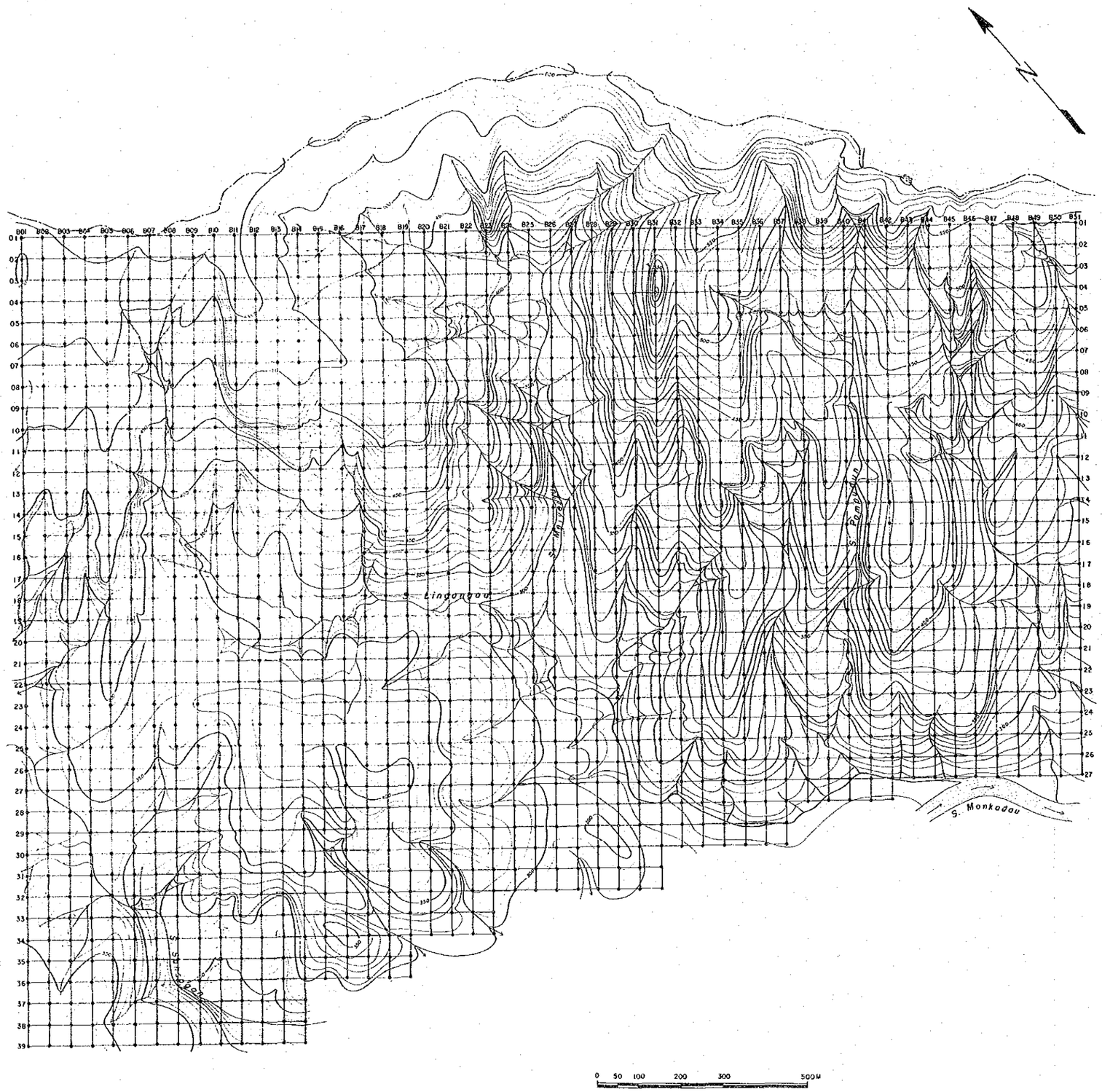

LEGEND

• Sample location and sample number

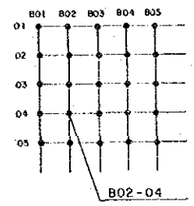

Fig. 61

Location Map of Soil Samples in "b" Area

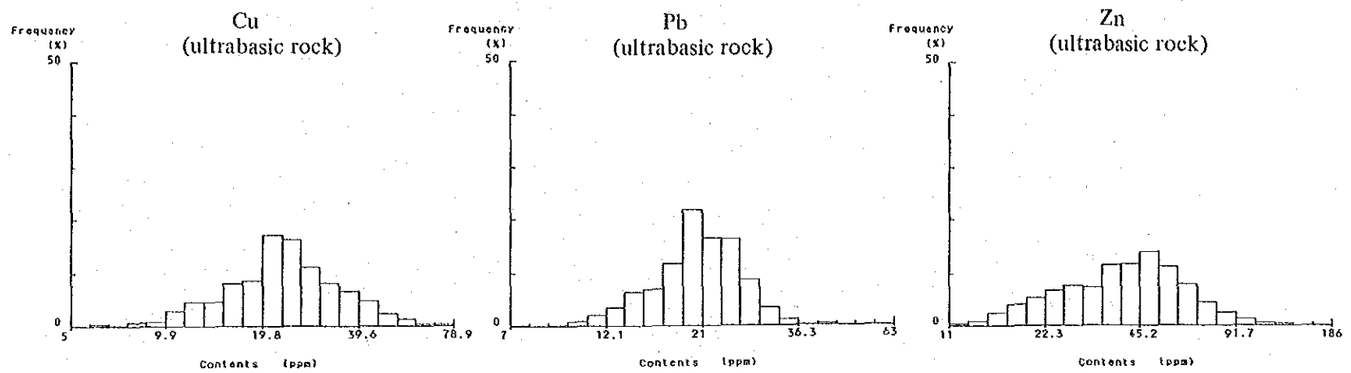

Fig. 62 Histgram for Soil Samples in "b" Area

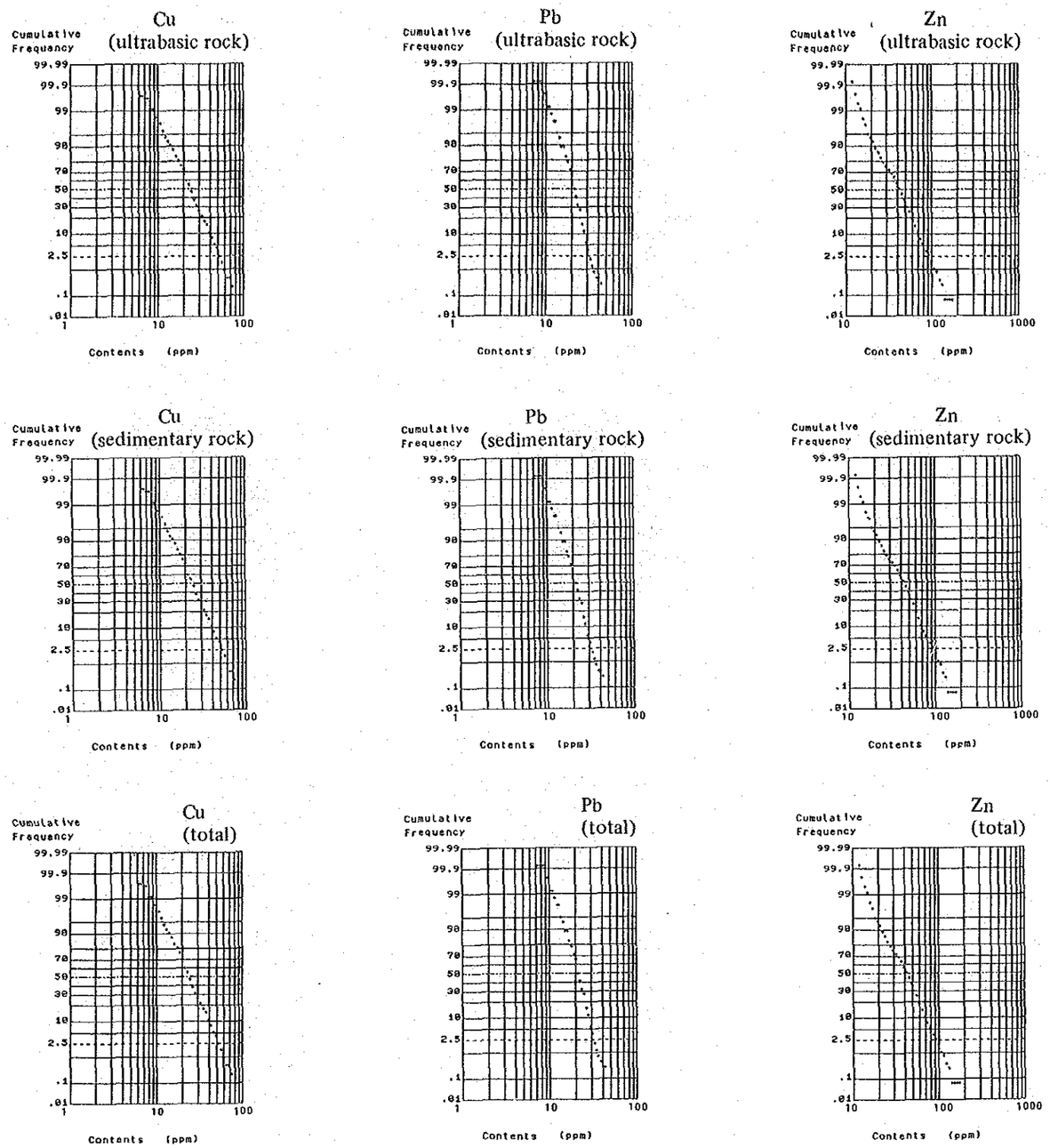

Fig. 63 Cumulative Frequency Curve for Soil Samples in "b" Area

assay values in the order of them. Then a straight line was drawn to pass each point plotted. Since the points adjacent to 50 per cent probability represent the greater part of the background population, consideration was given that the straight line does not fall apart from these points. The straight lines thus drawn are indicated by two curves or broken lines in general, which is not necessarily distinct in this data. Therefore, the distribution diagrams were produced based on the values of $\bar{X} + 2t$ which occupy about 2.5 per cent of the entire population. $\bar{X} + t$ and $\bar{X} + 3t$ were also used in the distribution diagrams as the supplementary values. These values are shown in Tables 9 and 10 for each area. Correlation between the elements are also shown in Table 11.

The distribution by element thus produced is shown on the 1 : 50,000 scale topographical maps (Map 13 – 15 and 18 – 22). Since the classification of the rock facies is shown on the distribution maps, they are treated as those distributed in each classified rock facies because of discontinuity of the boundaries of rock facies.

2–3–2 Multivariate Analysis

Score-sum (SCORESUM) and factor analysis are adopted for the method of multivariate analysis.

The contents are shown as in the following.

(1) Score Sum

Since the assay results of the samples provided for the analysis were relatively low in grade as shown at the end of this report (the maximum values of each element were 79 ppm Cu, 63 ppm Pb and 186 ppm Zn in the b area, and 462 ppm Cu, 601 ppm Pb, 282 ppm Zn, 11 ppm Mo and 0.72 ppm Au in the c area), it is difficult to extract the intrinsic geochemical anomalous zones.

It seems, however, that the procedure by score-sum is powerful for examining the potential of mineralization. The characteristics of the procedure are as follows.

- The kinds of geochemical data are not constrained.
- The number of the elements analyzed or the samples are not limited.
- Classification of rock facies can be easily reflected.
- Even the low anomalies can be accentuated.
- It is possible to delineate the outline of anomalous zones and they are easily to be ranked.
- Many data can be plotted on one or several sheets of diagrams.

It is thought that score sum is effective for the analysis of this area in the aspect that the anomalous zones can be extracted by a set of values even if a single element is low in grade, as mentioned in the above, and that the classification of rock facies can be considered.

Table 16 Statistic Values for Soil Samples in "b" Area

			Ultrabasic rock	Sedimentary rock	Total
Cu (ppm)	Number of samples	(n)	927	754	1681
	Maximum value	(Vmax)	79	72	79
	Minimum value	(Vmin)	6	5	5
	Geometric mean	($\bar{X}$)	23.1	15.2	19.2
	Standard deviation	(t)	0.178	0.226	0.220
	$10^{\log\bar{x}+t}$		34.8	25.6	31.9
	$10^{\log\bar{x}+2t}$		52.4	43.0	52.9
	$10^{\log\bar{x}+3t}$		(79.0)	(72.4)	(87.8)
Pb (ppm)	Number of samples	(n)	927	754	1681
	Maximum value	(Vmax)	63	43	63
	Minimum value	(Vmin)	7	7	7
	Geometric mean	($\bar{X}$)	16.2	20.5	18.0
	Standard deviation	(t)	0.119	0.110	0.120
	$10^{\log\bar{x}+t}$		21.3	26.4	23.7
	$10^{\log\bar{x}+2t}$		28.0	34.0	31.3
	$10^{\log\bar{x}+3t}$		36.9	(43.8)	41.2
Zn (ppm)	Number of samples	(n)	927	754	1681
	Maximum value	(Vmax)	186	92	186
	Minimum value	(Vmin)	14	11	11
	Geometric mean	($\bar{X}$)	49.7	29.7	39.4
	Standard deviation	(t)	0.148	0.185	0.200
	$10^{\log\bar{x}+t}$		69.9	45.5	62.4
	$10^{\log\bar{x}+2t}$		98.2	69.6	99.0
	$10^{\log\bar{x}+3t}$		138.2	(106.6)	156.9
Mo (ppm)	Number of samples	(n)	927	754	1681
			All data show the values below detection limit.		

note) ( ) ; value not present

Correlation Matrix

	Ultrabasic rock			Sedimentary rock			Total		
	Cu	Pb	Zn	Cu	Pb	Zn	Cu	Pb	Zn
Cu	1	–	–	1	–	–	1	–	–
Pb	0.317	1	–	0.301	1	–	0.086	1	–
Zn	0.486	0.148	1	0.853	0.286	1	0.753	–0.067	1

The method of analysis is as follows.

(i) The values of $\overline{X} + t$, $\overline{X} + 2t$ and $\overline{X} + 3t$ are calculated for each rock facies used in simple statistical analysis.

(ii) Scores are given to each class established on the basis of the values calculated in the above.

Class	Score
less than $\overline{X} + t$	0
$\overline{X} + t \sim \overline{X} + 2t$	1
$\overline{X} + 2t \sim \overline{X} + 3t$	2
larger than $\overline{X} + 3t$	3

(iii) The score of the sample is determined by totaling the score of each element for each sample.

(iv) As a result, the anomalous zones are ranked by these scores, in which score 9 is the maximum in the case of analysis of these components (all three components show the values larger than $\overline{X} + 3t$).

The results are described on geological map, and geochemical anomalies were extracted after examining the relationship with the result of geological mapping.

(2) Factor Analysis

The factor analysis, on the other hand, was introduced for the c area to grasp the behavior of elements.

The technique basically involved establishing a smaller number of provisional variables called factors from a large number of variables. By quantifying the degree of association each sample has to a factor, that is, by giving it a factor score, it is possible to describe spatially the relationship of the samples to each factor. Each factor, in the case of geochemical values, probably represent a type of mineralization, lithology and so on, in which carious elements are closely associated.

In this procedure, the examination was made on both cases of classified and unclassified rock facies, and the classification of rock facies was also investigated.

These works were treated by varimax method using computer.

2–4 Result of Survey

The distribution of each of the three elements such as copper, lead and zinc out of five elements chemically analyzed was indicated on the geologic maps (1 : 50,000 in scale). Molybdenum could not be the objective of analysis because all the assay values were below the detection

limit (1 ppm). Gold was also excluded from the objective of this time because the chemical analysis was made only for selected samples.

The three elements excepting molybdenum and gold were expressed on the 1 : 50,000 scale geologic map as the score sum map, and the evaluation was given by the scores at the sampling position.

2–4–1 Distribution of Elements

(1) Copper (Cu)

The distribution of Cu is shown on Map 38. The maximum assay value is 79 ppm and the minimum 5 ppm, being low in general.

Since the distribution of assay values is different for each rock facies, they were roughly divided into peridotite and the sedimentary rock facies.

As a result, the widest zone showing the values larger than $\overline{X} + 2t$ is shown in the vicinity of B23–02, corresponding to the distribution of basalt, having a tendency to extend beyond the boundary of the survey area.

The values larger than $\overline{X} + 2t$ are also scattered in the terrain of peridotite in the northeastern part of the survey area.

(2) Lead (Pb)

The distribution of Pb is shown on Map 39.

The maximum assay value is 63 ppm and the minimum 7 ppm. The rock facies was divided in the same way as in the case of Cu. The average value is higher in the sedimentary rock facies than in peridotite.

The distribution shows a tendency to extend northeasterly in the northwestern part and the central part of the survey area. This trend is almost consistent with the direction of the rivers, seemingly reflecting the influence of it.

The values larger than $\overline{X} + 2t$ are distributed in the peridotite having a lateral extent of 2,250 m^2, showing a tendency to extend northward beyond the boundary of the survey area.

(3) Zinc (Zn)

The distribution of Zn is shown on Map 40.

The maximum assay value is 186 ppm and the minimum 11 ppm, and the aspect of distribution is greatly different for each rock facies. The average values were 49.7 ppm in the peridotite, whilst 29.7 ppm in the sedimentary rock facies, showing low value in the latter.

In connection with the values of $\overline{X} + t$, they are homogeneously distributed throughout the survey area, and it is evident that those of $\overline{X} + 2t$ are distributed in the sedimentary rock facies

in the northwestern part of the survey area and in the basalt terrain in the northeastern part.

The values larger than X + 2t found in the vicinity of B23–01 corresponds to the distribution of basalt showing a tendency to extend northeasterly beyond the boundary of the survey area. Those in the vicinity of B01–35, B02–04, B05–32, B23–01 and B40–23 are well consistent with the xones of X + 2t of Cu.

2–4–2 Result of Analysis by Score Sum

The result of analysis by score sum is shown on Map 41.

The highest score in the map was five. The score of five means that in each of the rock facies classified, at least one element among the three elements of Cu, Pb and Zn contains the value larger than $\bar{X}$ + 2t.

This is the same as for score four. Therefore, the distribution will be considered up to four of the score.

The number of positions in the survey area where the samples of scores of four or five were collected are 24. Among these, 10 are found in the terrain of peridotite and 14 in that of sedimentary rock facies. The ratio of numbers of these samples to the whole number of samples in each rock facies are 1.08 per cent in the case of peridotite and 1.86 per cent in the case of sedimentary rock facies. When the sedimentary rock facies is divided into sandstone and basalt, the ratios are 30.0 per cent and 1.09 per cent respectively.

Thus it was made clear that basalt held the first priority from the standpoint of rock facies. It must be noted, however, that the number of samples collected in the basalt terrain is scarce and that basalt was treated as the sedimentary rock facies collectively because it belongs to the same formation as the sedimentary rocks.

On the other hand, the high score (four and five in score) zone is classified into the zones form I to V. These zones show the following characteristics.

Zone I : Situated at the northern end of the survey area, and distributed on the slope near the ridge in the N-S direction. The rock consists of peridotite.

Zone II : Situated in the northwestern part of the survey area, and distributed in the area where the slope varies its inclination. The rocks consist of peridotite and sandstone and they are in a fault contact with each other in the E-W direction.

Zone III : Situated at the western end of the survey area and distributed on a relatively gentle hill. The rock consists mainly of sandstone, in which west-northwesterly trending faults are found.

Zone IV : Distributed at the northeastern end of the survey area associated with basalt. Topo-

graphically, the zone occupies the very steep southwestern slope, and the faults in the east-northeastern trend and the west-northwestern trend control the boundaries of basalt.

Zone V : Located at the end of the relatively gentle slope in the southeastern part of the survey area. The rock consists of sandstone.

From the above, it can be assumed that the distribution of the high-score zones was influenced by the rock facies represented by the Zone IV or that it was controlled by the structures including the faults represented by the Zone II and Zone III. The Zone I and Zone V are not necessarily consistent with such geological environments.

2–5 Discussion

Regarding the five zones extracted by the score sum method, discussion is made on the possibility of extracting geochemical anomalous zones taking the alteration zones and mineralized zones obtained as a result of geological mapping into account.

Fig. 64 (Map 42) is utilized as the diagram for analysis.

The characterisitcs of the zones are as follows.

Zone I : The distribution is consistent very well with that of lateritic soil in the peridotite. Cu and Pb anomalies were obtained by statistical treatment of the geochemical survey data.

Zone II : The distribution is consistent with the spread of lateritic soil found in the area where peridotite is in a fault contact with sandstone. The geochemical survey resulted in to detect the anomalies of three elements such as Cu, Pb and Zn.

Zone III : The distribution is consistent with the weakly argillized zone in sandstone developed along the fault. Although the geochemical survey resulted in to detect the anomalies of Cu, Pb and Zn, their assay values are relatively low.

Zone IV : The zone is found in the basalt terrain, and overlaps with the occurrence of lateritic soil and argillized zone. The geochemical survey detected the anomalies of Cu and Zn, but no Pb anomaly was detected.

Zone V : The zone is distributed in sandstone, and the relationship with alteration and mineralization is indistinct. Correlation with structural factors including fault can not also be made clear. Geochemical survey detected the anomalies of Cu, Pb and Zn.

From the above, Zone I, Zone II and Zone IV might be extracted as the geochemical anomalous zones. All these are considered to be closely associated with lateritic soil. However, it should be noted that these zones are different in their characters because these anomalous zones have different characteristics of rock facies and structure and because of different combination of elements which showed the anomalous values. On the other hand, Zone III appears to be a local

anomaly along the fault, showing relatively low anomalous values.

As to Zone V, relationship with alteration and mineralization obtained from geological mapping is indistinct, leading to make judgement difficult at the present stage.

The geochemical survey resulted in detection of no anomalies as to the floats of massive sulfide ore distributed along the Lingangaa Creek.

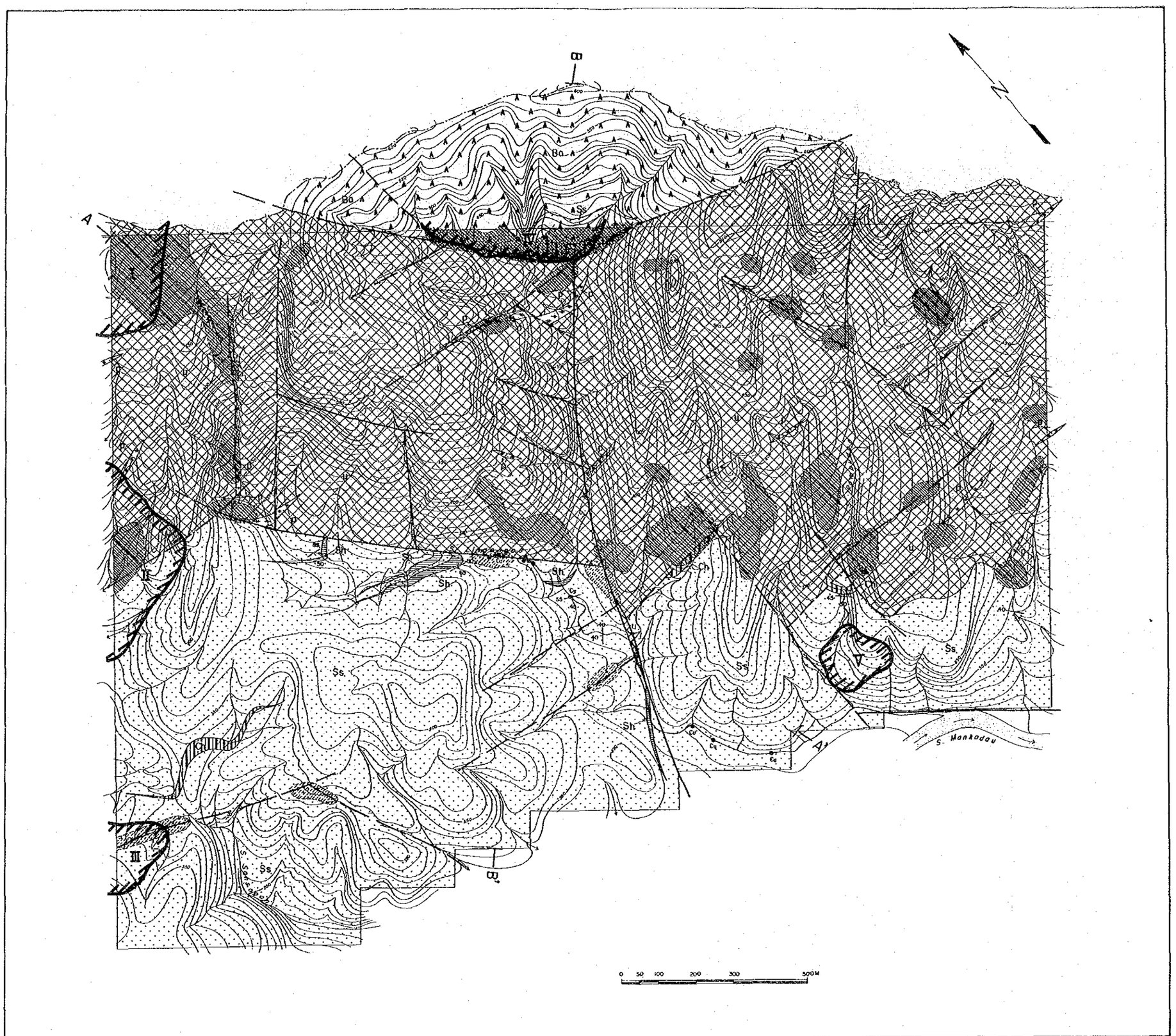

LEGEND

anomalous zone

Trusmadi Formation

Ss sandstone
Ch chert
Sh shale
Bc basalt

Intrusive Rocks

P pegmatite
U ultrobasic rock

Fault(certain)
Fault (inferred)
Strike and dip
A—A' Geological Profile line

lateritic soil
argillized soil
lateritic and argillized soil
Cu float of copper boulder
Cr float of chromite boulder

Fig. 64

Geochemical Interpretation Map of "b" Area

Chapter 3 Geophysical Survey (CSAMT Method)

3–1 Objectives and Specifications

The same CSAMT method as in the "A" area was carried out in the "B" area in order to clarify the underground resistivity structure and to select the most promising potential area for the porphyry copper type ore deposit.

Table 17 shows the details of the survey amounts and specifications and Map 42 gives the location of survey stations.

Table 17 Specifications and Survey Amount for CSAMT Survey in "b" Area

Number of stations	203 points
Station spacing	400–500 m
Electrode separation	Tx3 2,000 m Tx4 2,000 m
Area covered	100 sq. Km

Data processing and analysis were made the same methods as described in 2–1–2 ("A" area).

3–2 Survey Results

3–2–1 Apparent Resistivity Plan Map

In this area, the topographic change is controlled by a dominant NW-SE trending structure having a steep topography in the north-western part of the area. In order to interpret the results obtained in this area, it was adopted the same frequency range as one in the "A" area. Apparent resistivity maps are shown in Figs. 65–69 and Maps 44–53.

The apparent resistivity obtained in the high frequency range reflect the shallow information. However, the pattern distribution happened to be almost the same as that of the low frequency range.

The apparent resistivity in the lower frequency range is comparatively low showing a tendency of expanding its low resistivity zone at depths.

(1) A low resistivity of less than 50 ohm-m is distributed dominantly in the area, and high resistivities of more than 100 ohm-m are seen both in the center and in the northeastern end of the surveyed area, splitting the above mentioned low resistivity zone.

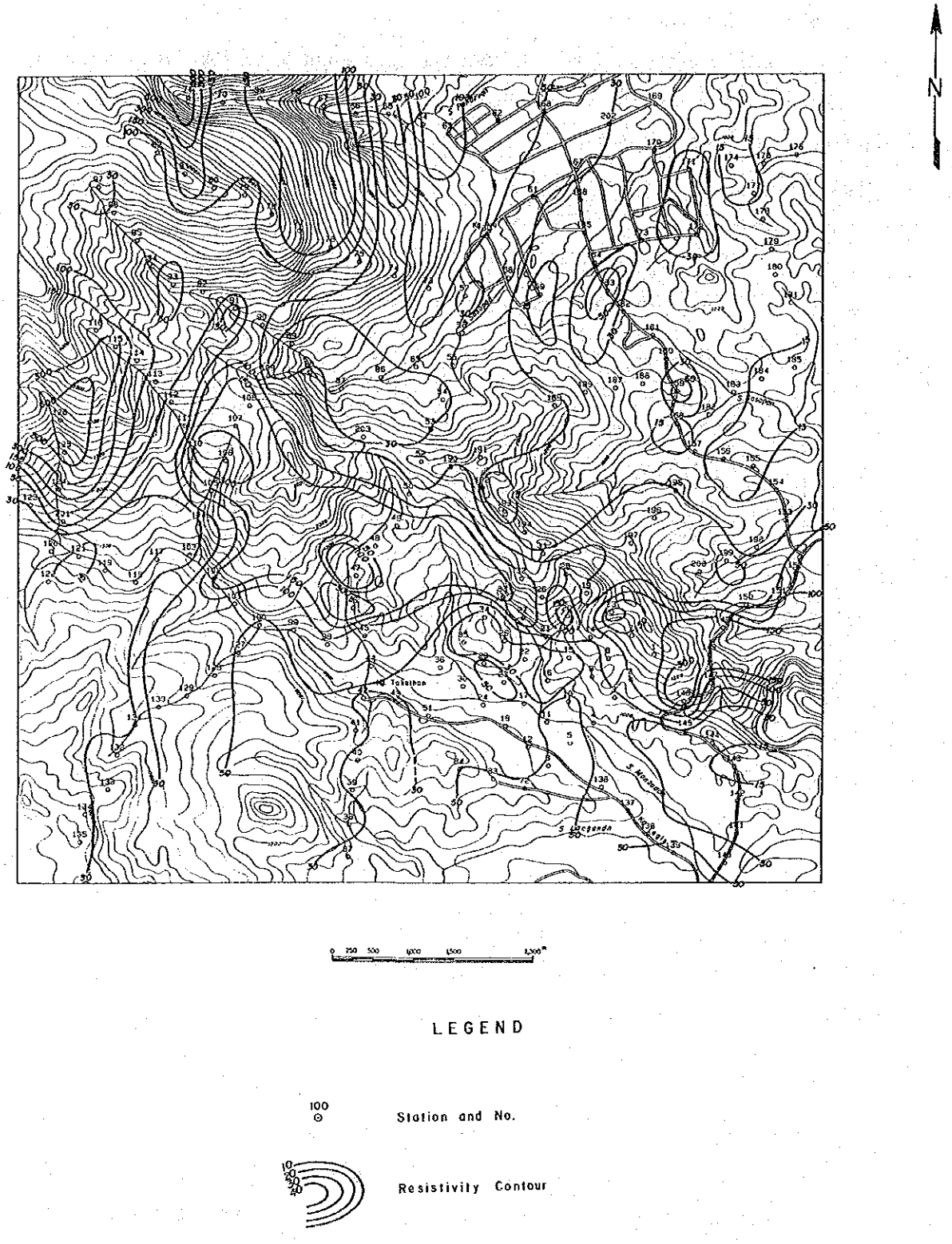

Fig. 65 Apparent Resistivity Plan Map in "B" Area (2048 Hz)

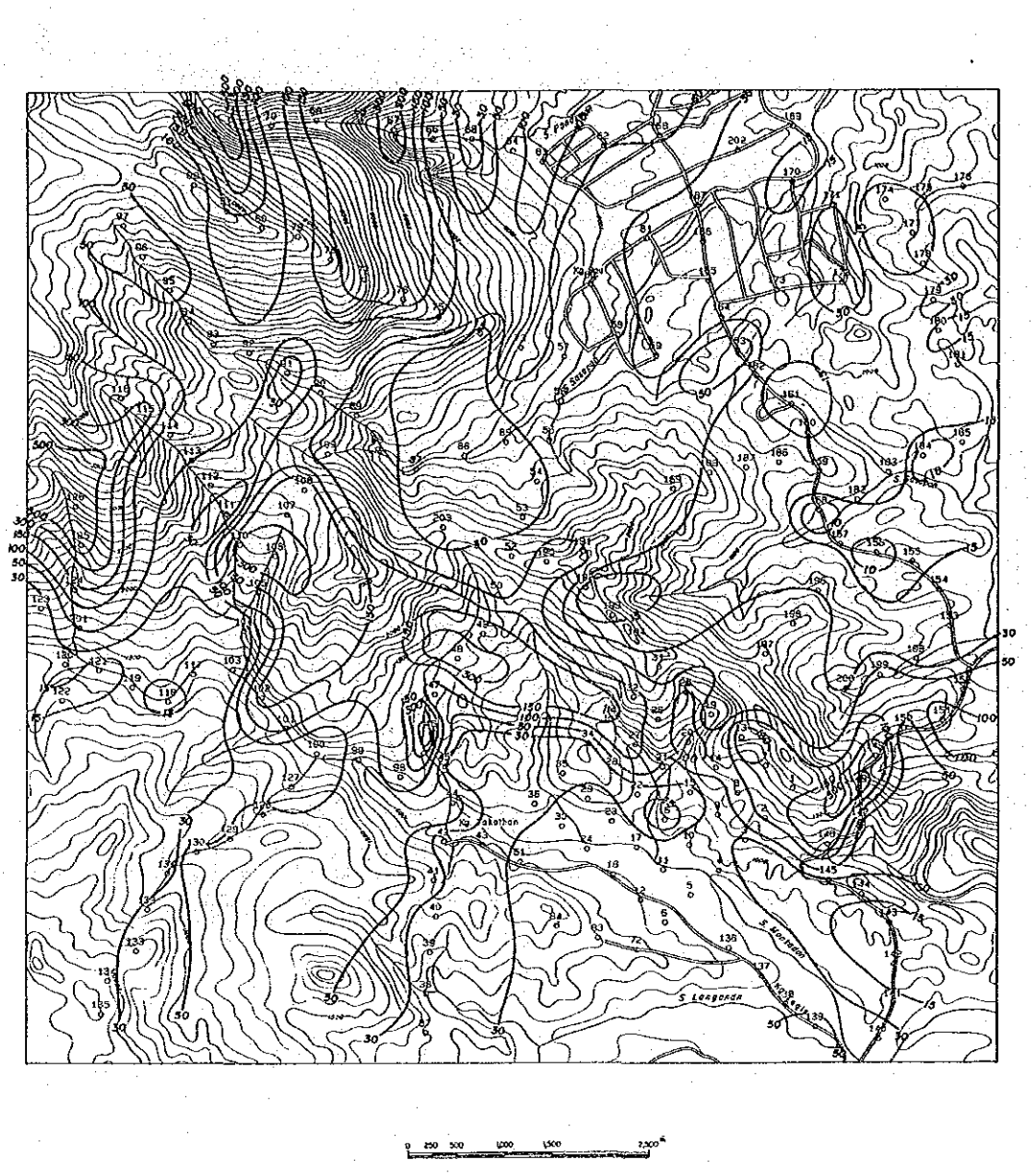

Fig. 66 Apparent Resistivity Plan Map in "B" Area (1024 Hz)

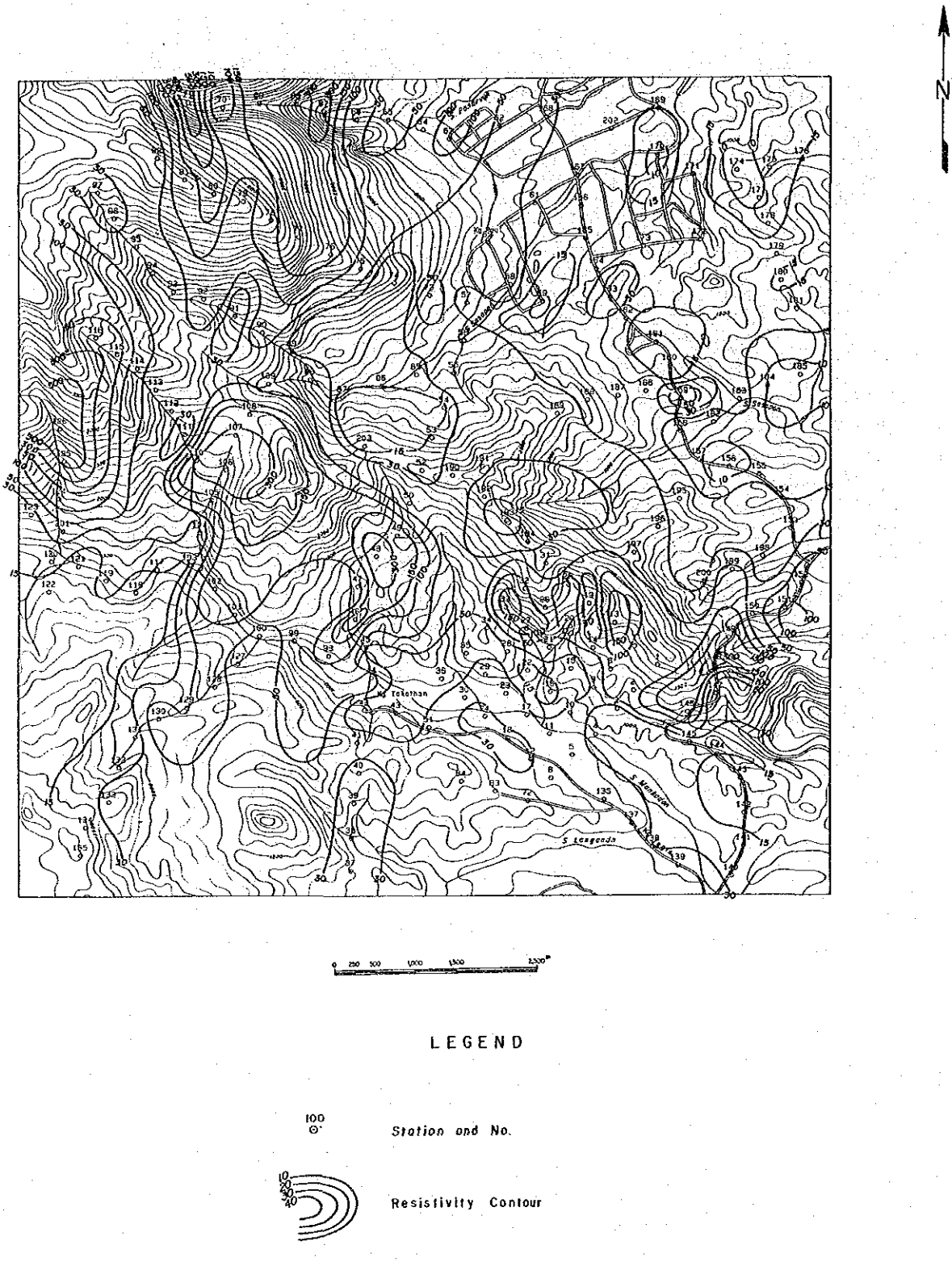

Fig. 67 Apparent Resistivity Plan Map in "B" Area (512 Hz)

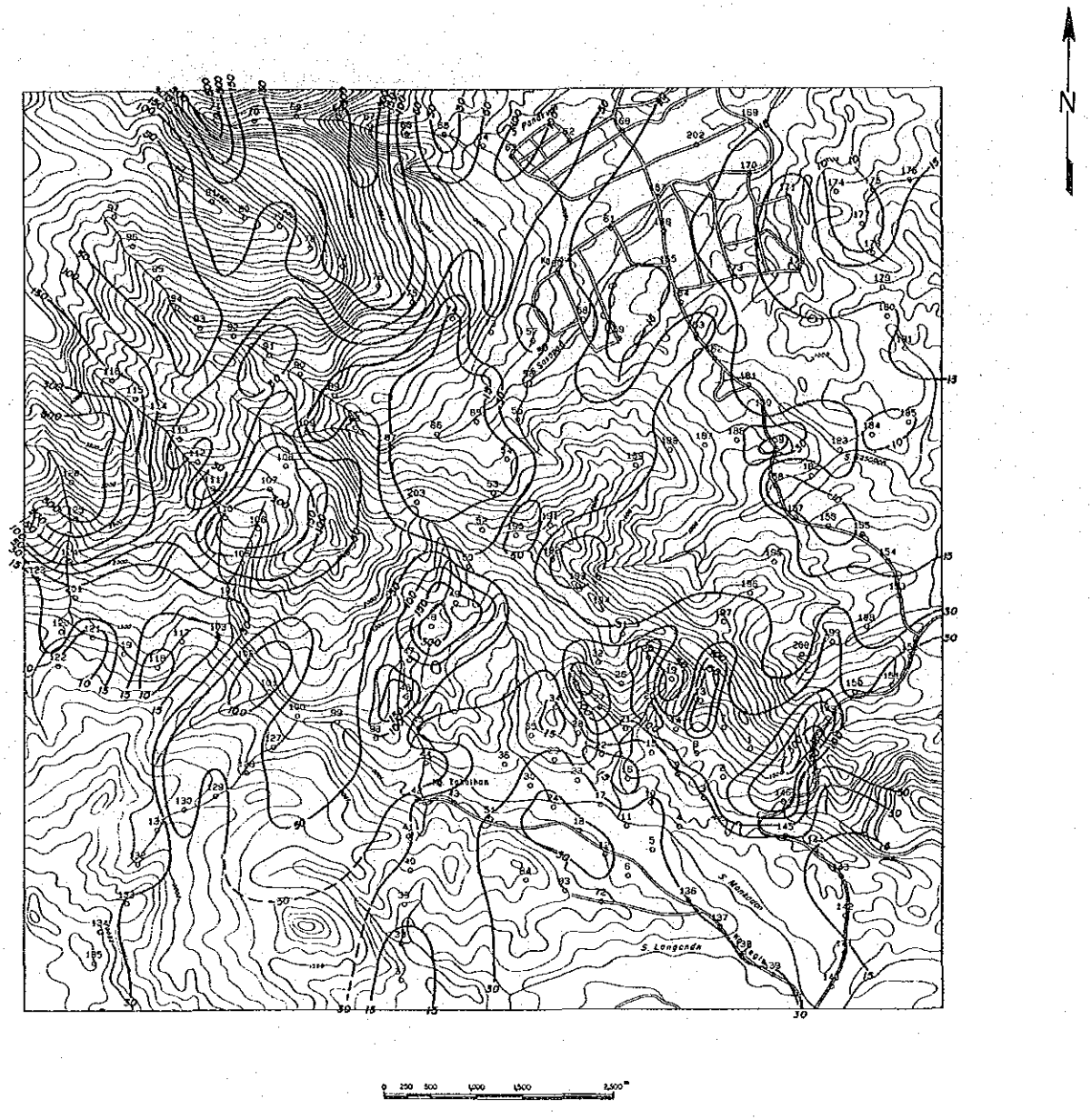

Fig. 68 Apparent Resistivity Plan Map in "B" Area (256 Hz)

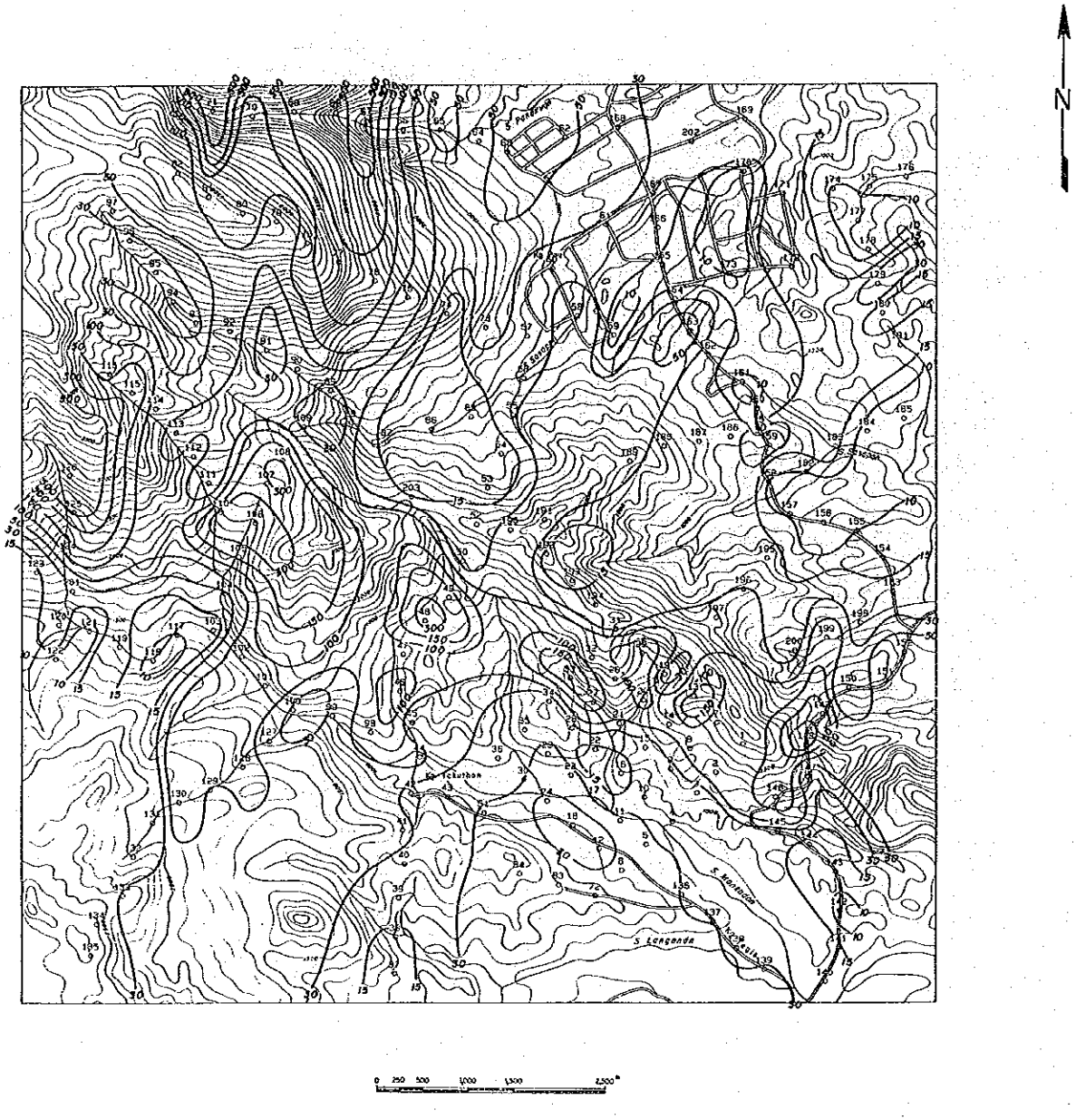

Fig. 69 Apparent Resistivity Plan Map in "B" Area (128 Hz)

(2) Apparent resistivity of more than 100 ohm-m is partly seen in the center of the area, owing to the local compact rock. It shows a tendency to continue in the NW-SE direction.

The discontinuity in the resistivity may be due to the faults with a complex geological structure. The block distribution, controlled by several faults, can be clearly seen in the deeper frequency range.

The resistivity change detected in the northwestern end of the area is monotonous from the surface to the depths, suggesting that it may be due the massive resistive body. This high resistive zone, detected in both areas, with a resistivity of more 100 ohm-m must be due to the same kind of rock corresponding well with the distribution of the peridotite.

(3) Low resistivities of less than 30 ohm-m are detected in the four areas: northeast, center, southeast and southwest of this are being widely extended from the surface to the depths.

Among them, the lower resistivity is seen in the northeastern part of the area, with a lowest value of less than 10 ohm-m and forming a big scale conductive anomaly zone, which becomes into one in the center of the area about 240 m below the surface.

(4) A resistivity of less than 30 ohm-m is detected in the southeastern and southwestern ends of the area, being extended monotonously from the surface to the depths in a similar way as the one detected from the northeastern to the center of the area.

Among the anomalies, the one observed in the southeastern part is detected as three independent resistivity distributions in the high frequency range, however, in the lower frequency range of less than 256 Hz, a continuous "mountain" shape resistivity zone was confirmed. It is inferred to be due to the fault and its fracture zone.

(5) A resistivity of about 100 ohm-m are scattered over the area in a small scale, being interpreted as thick Trusmadi formation.

3–2–2 Apparent Resistivity Sections.

Three apparent resistivity sections are shown in Figs. 70–72.

For each section, it can be seen a more predominant change of the resistivity in the horizontal than in the vertical direction, suggesting a simple layered structure.

Section E

This is a N-S trending section in the center of the area. Near Nos. 50 to 46, a high resistivity layer caused by thick peridotite is detected. This peridotite, being divided by the faults, is considered to be a massive body without any alteration. In spite of that, an extremely low resistivity was detected near the faults, reflecting the strong alteration.

On either side of the fault, a resistivity of less than 50 ohm-m is seen, suggesting the mono-

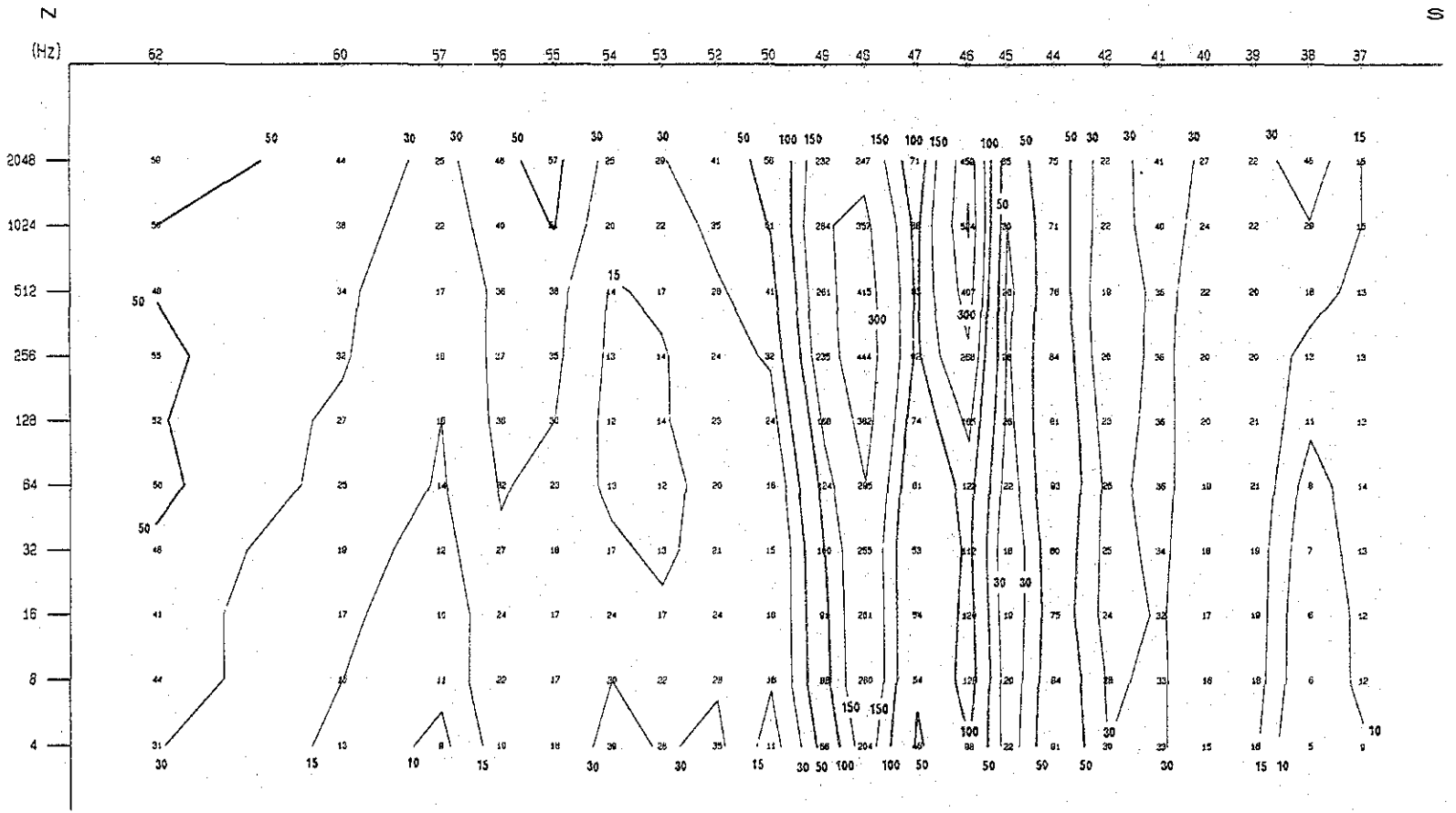

Fig. 70 Apparent Resistivity Section in "B" Area (Section E)